



SERS and SEIRA Signal optimisation and applications

Marc Lamy de la Chapelle

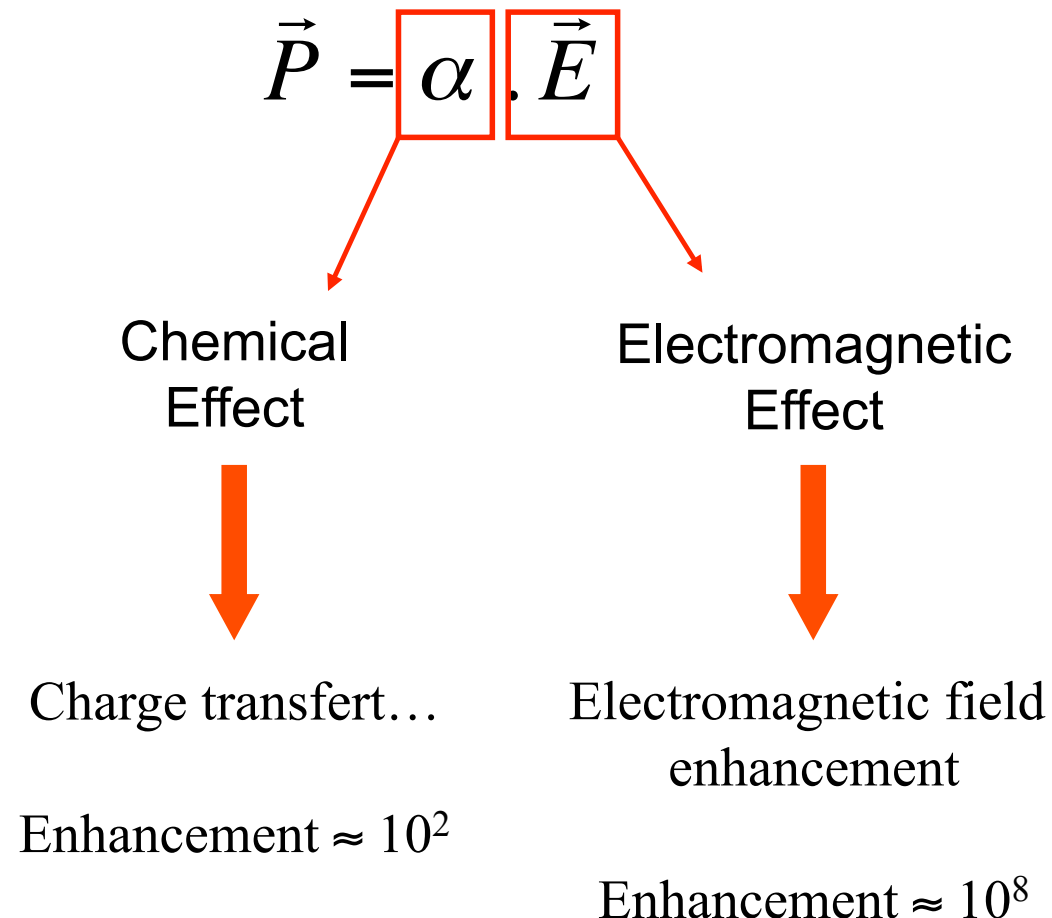
Laboratoire CSPBAT UMR7244, UFR SMBH, Université Paris XIII,
74 rue Marcel Cachin, 93017 Bobigny, France
email: marc.lamydelachapelle@univ-paris13.fr

Plan du cours

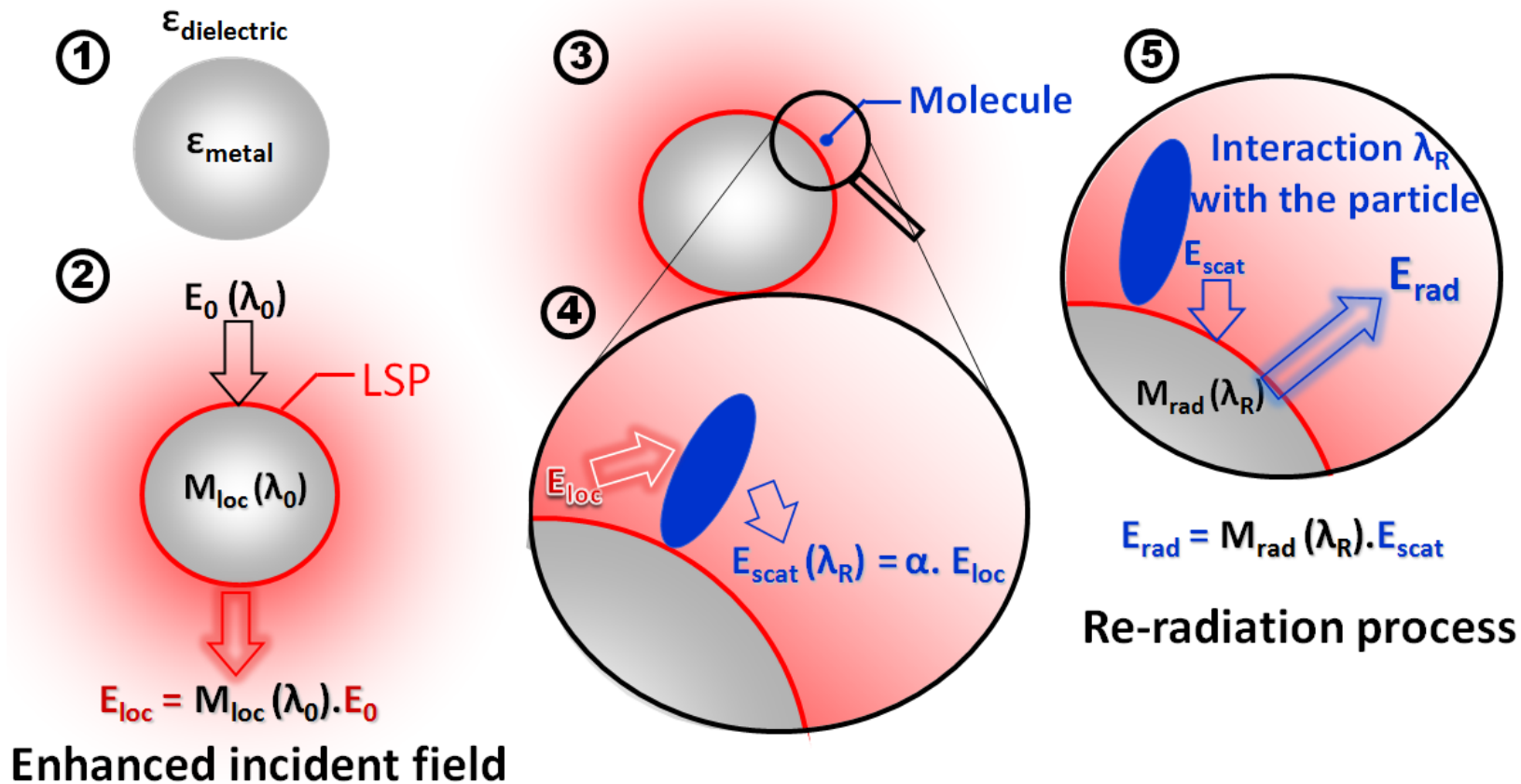
1. SERS signal optimisation
2. SERS sensor
3. SEIRA
4. SERS/SEIRA coupling

Signal optimisation in SERS

SERS principle



SERS principle: Electromagnetic effect

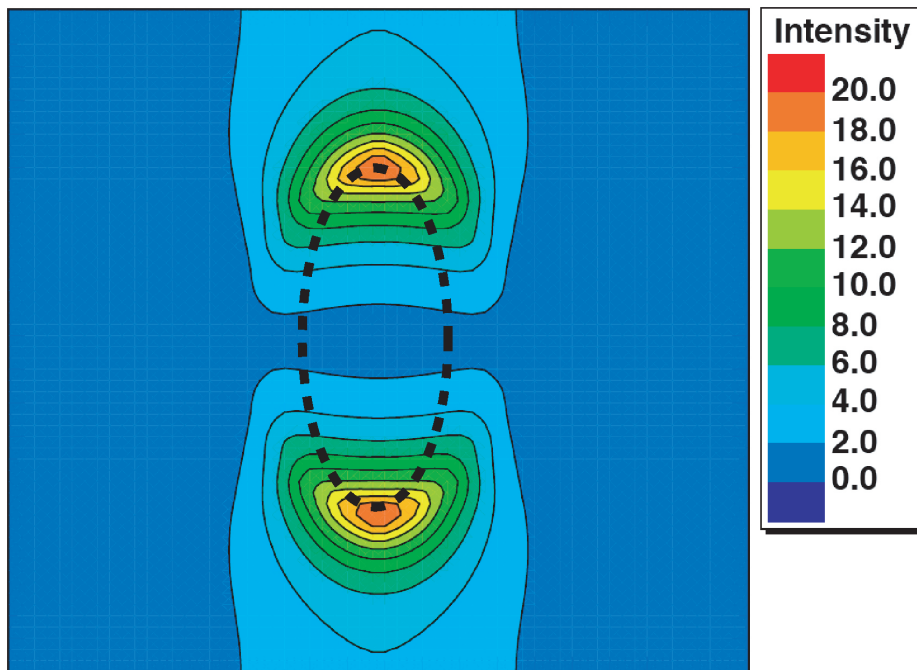


$$I_{\text{SERS}} = [M(\lambda_R) \cdot M(\lambda_0)]^2 \cdot \alpha^2 \cdot E^2$$
$$I_{\text{SERS}} = [M(\lambda_R) \cdot M(\lambda_0)]^2 \cdot I_{\text{Raman}} \approx M(\lambda_0)^4 I_{\text{Inc}}$$

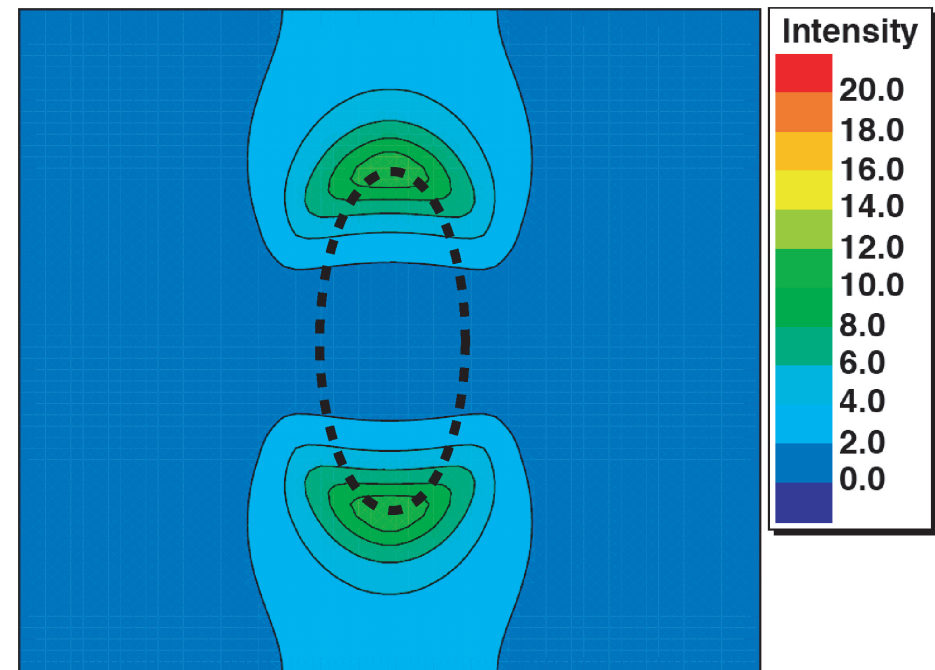
⇒ Giant Raman enhancement up to 10^{10}

Near field enhancement

Gold nanowire : long axis = 150 nm

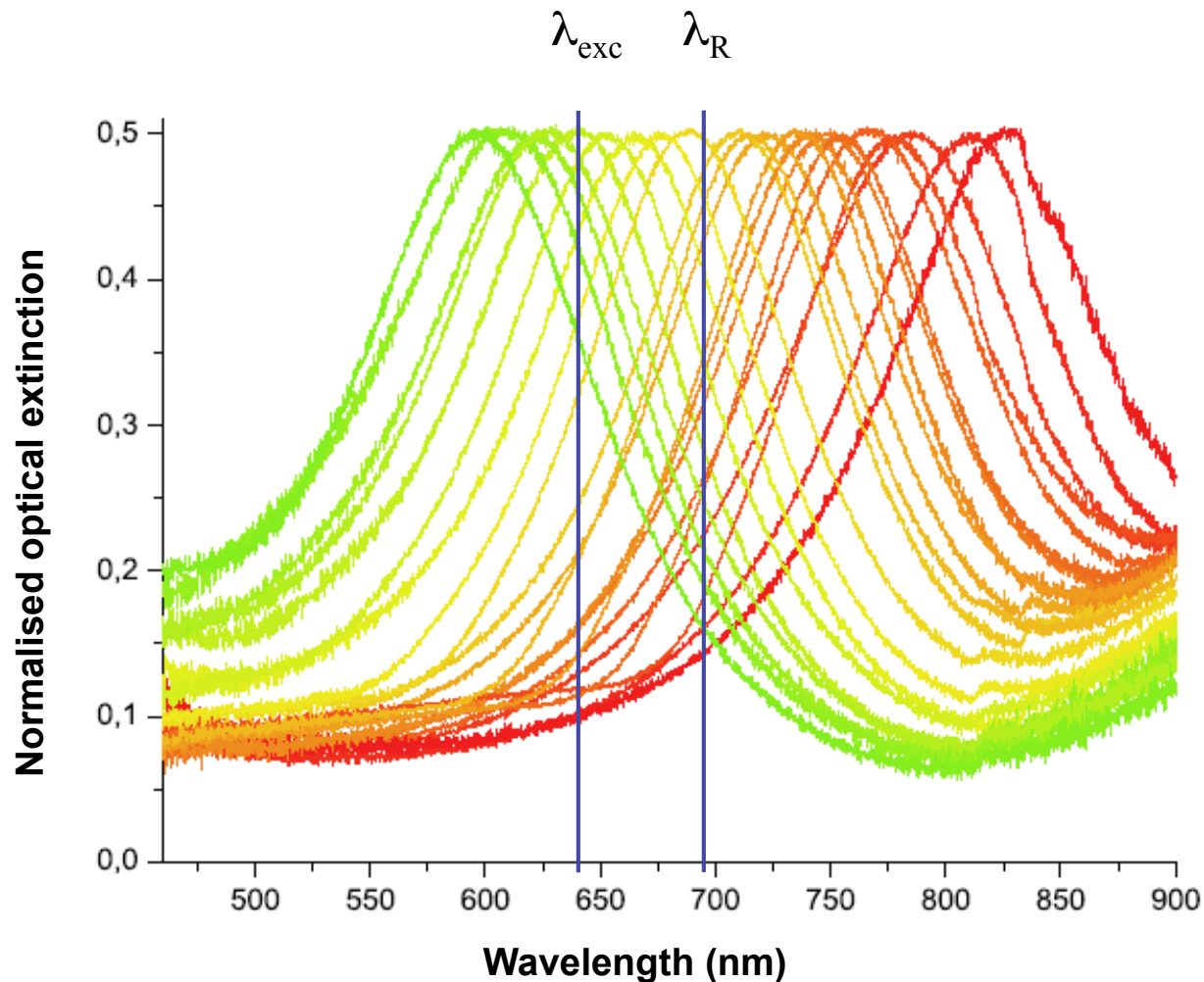


Intensity map at 712 nm

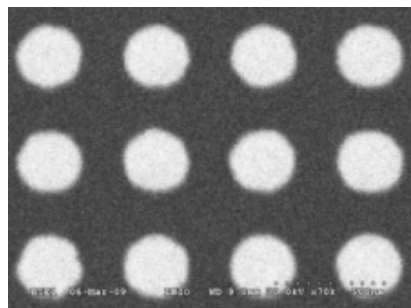


Intensity map at 800 nm

SERS Experiments



SERS Experiments



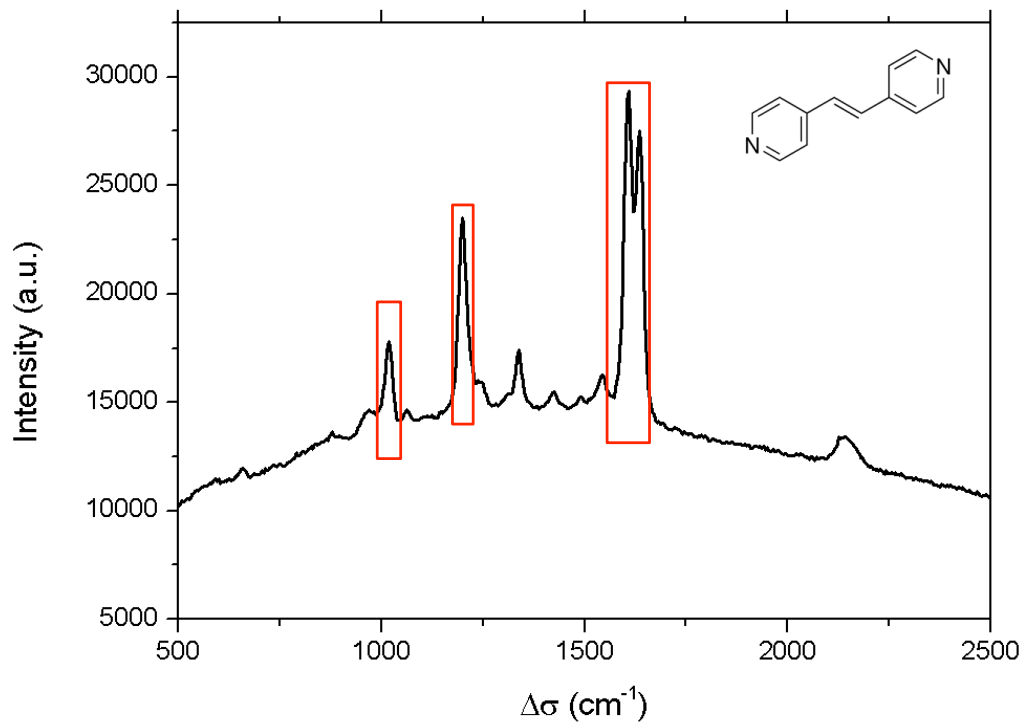
Nanocylinders :
 $100 \text{ nm} < \varnothing < 200 \text{ nm}$,
height = 50 nm

$$\lambda_{\text{exc}} = 633 \text{ nm}$$

$$\lambda_{\text{exc}} = 660 \text{ nm}$$

$$\lambda_{\text{exc}} = 691 \text{ nm}$$

$$\lambda_{\text{exc}} = 785 \text{ nm}$$



***trans*-1,2-bis(4-pyridyl)ethylene (BPE)**

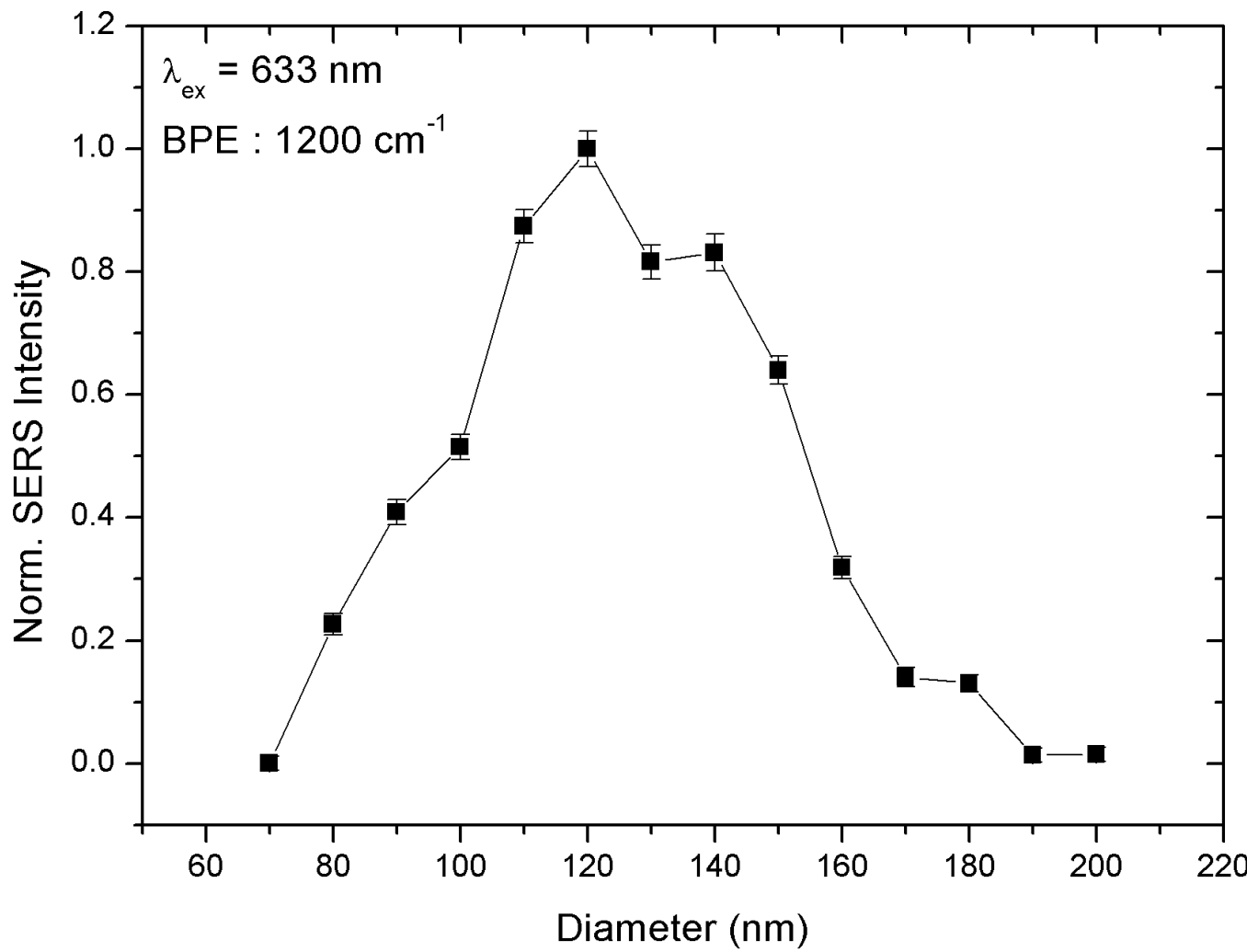
1007 cm^{-1} : pyridine ring breathing mode

1200 cm^{-1} : C=C stretching mode

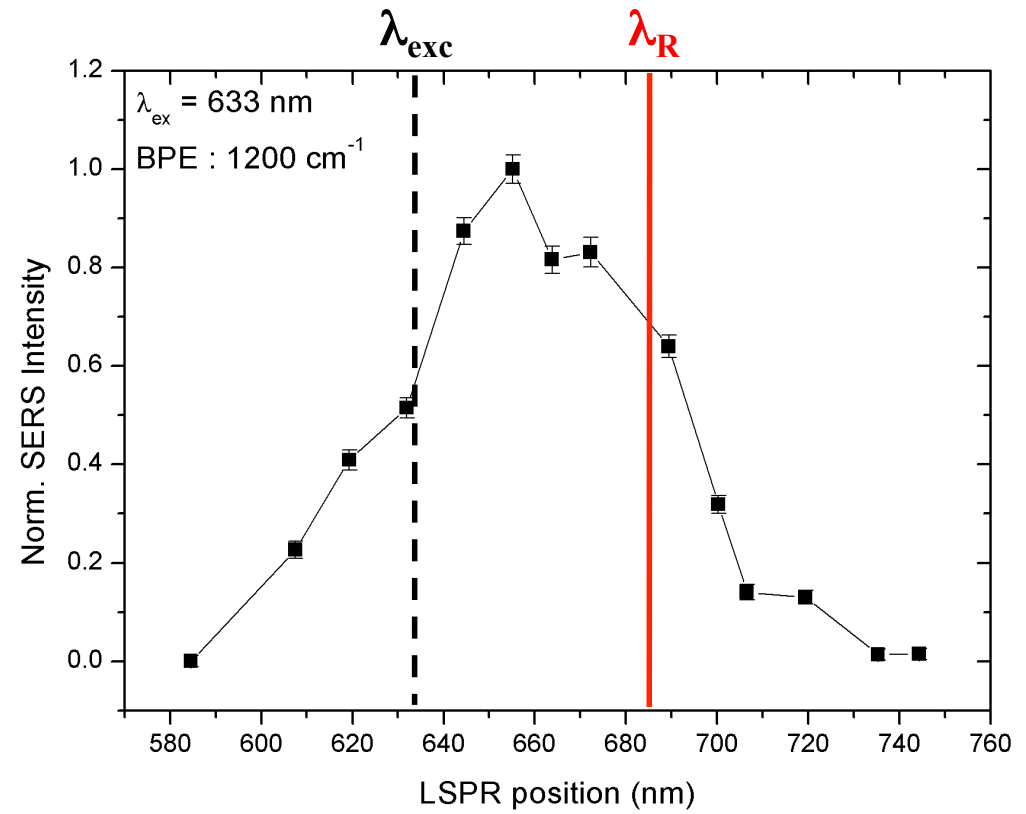
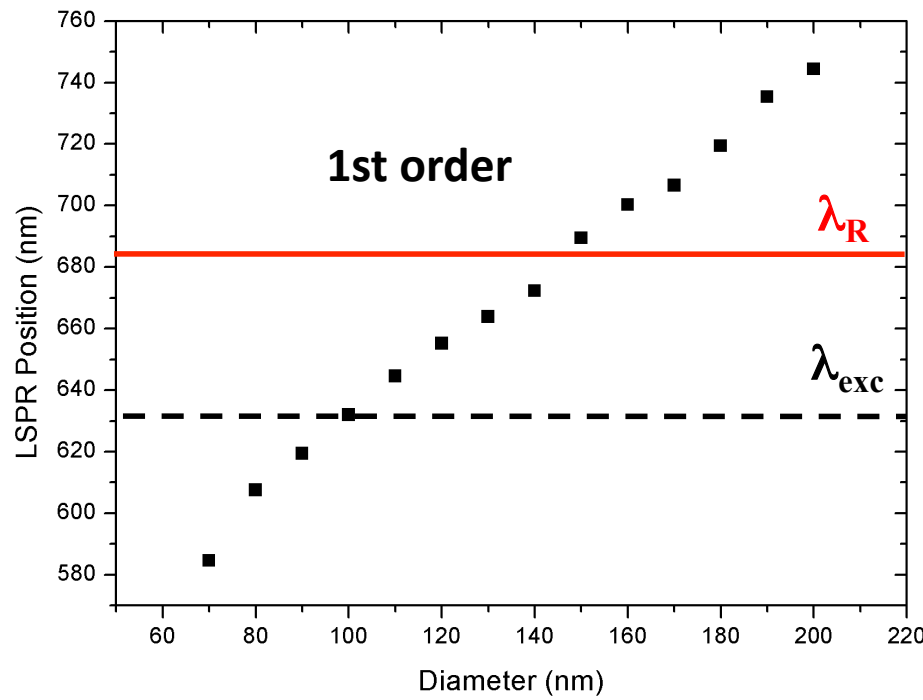
1606 cm^{-1} : pyridine ring C=C stretching mode

1636 cm^{-1} : whole pyridine ring stretching mode

SERS vs diameter



SERS vs LSPR



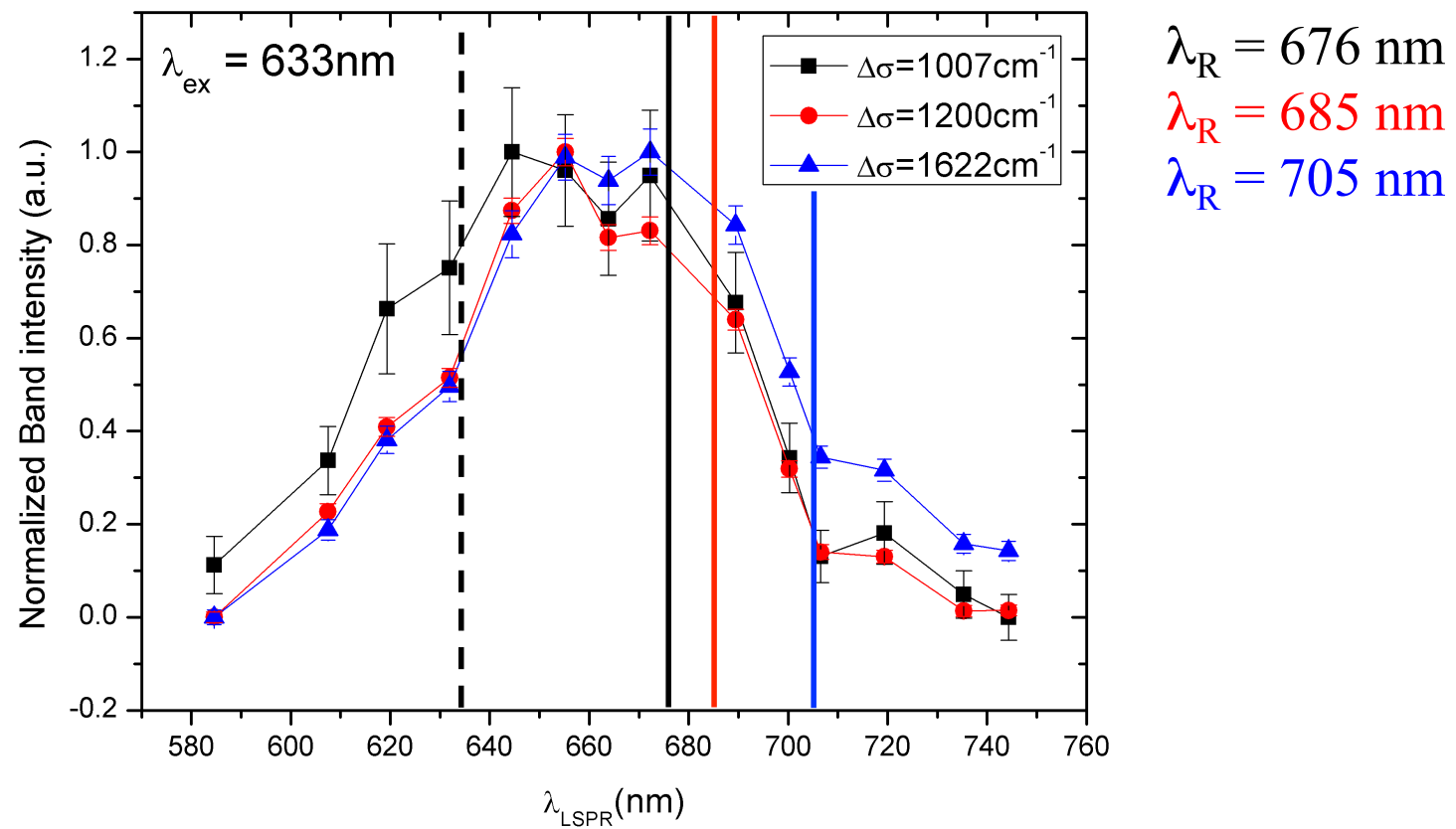
$$G_{SERS} = |f(\lambda_{exc}) \cdot f(\lambda_R)|^2$$

$$G_{SERS} \text{ Max} \Rightarrow \lambda_{exc} < \lambda_{LSPR} < \lambda_R$$

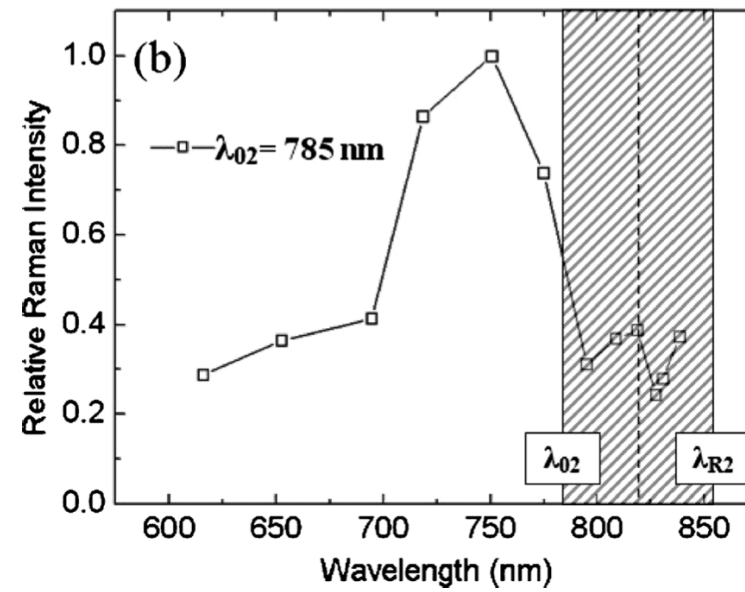
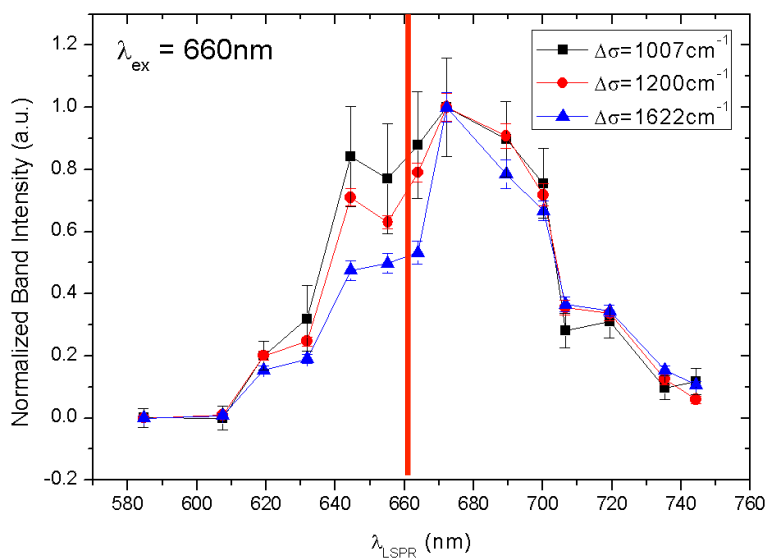
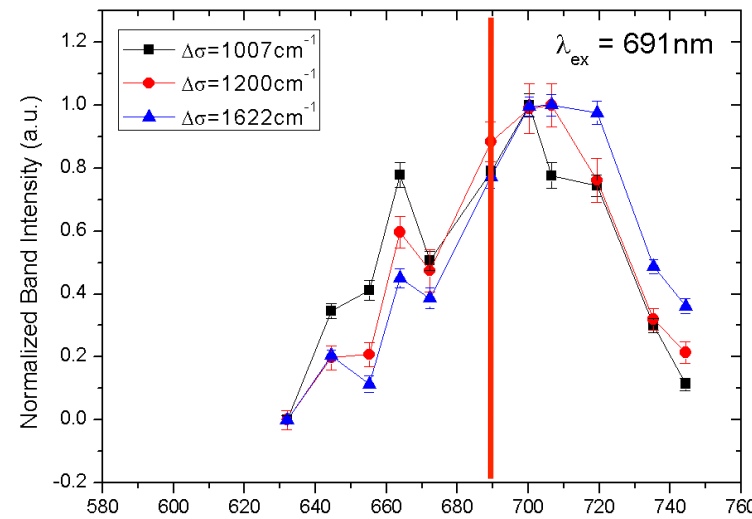
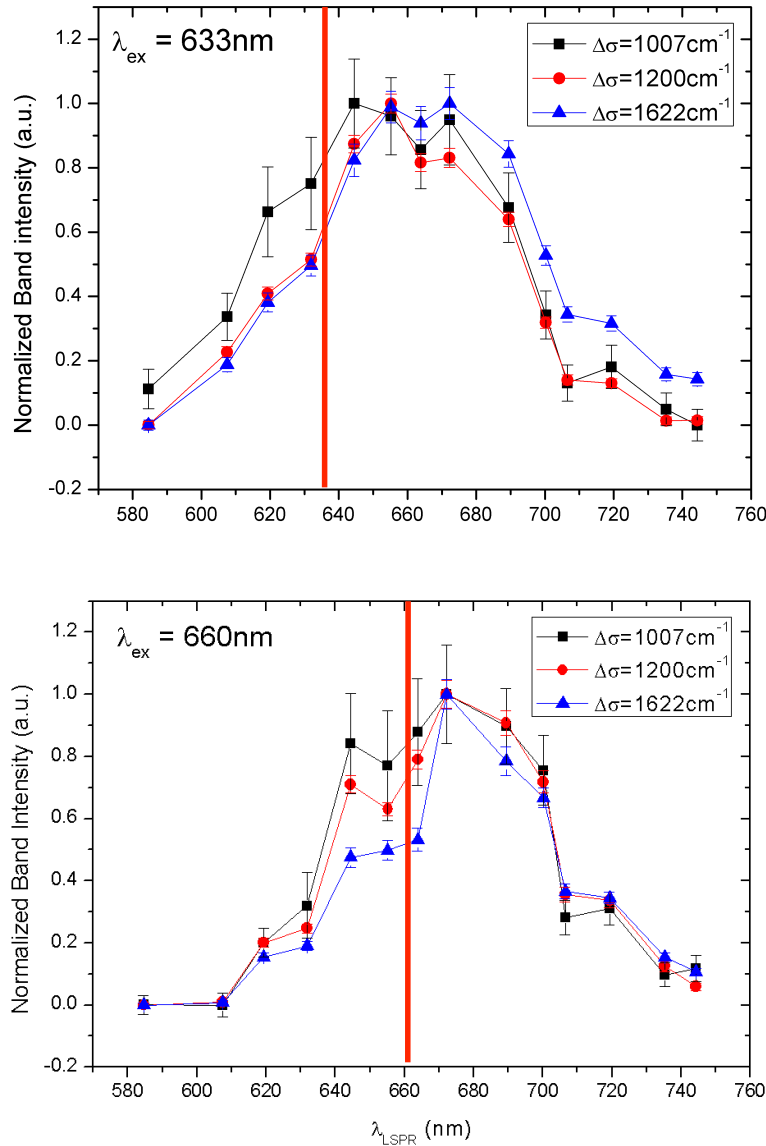
A.Wokaun *et al.*, *Solid State Phys.* 38, 1984

N. Guillot *et al.* *JQSRT* 113, 2321, 2012, N. Guillot *et al.*, *J. of Nanophotonics*, 6(1), 64506, 2012

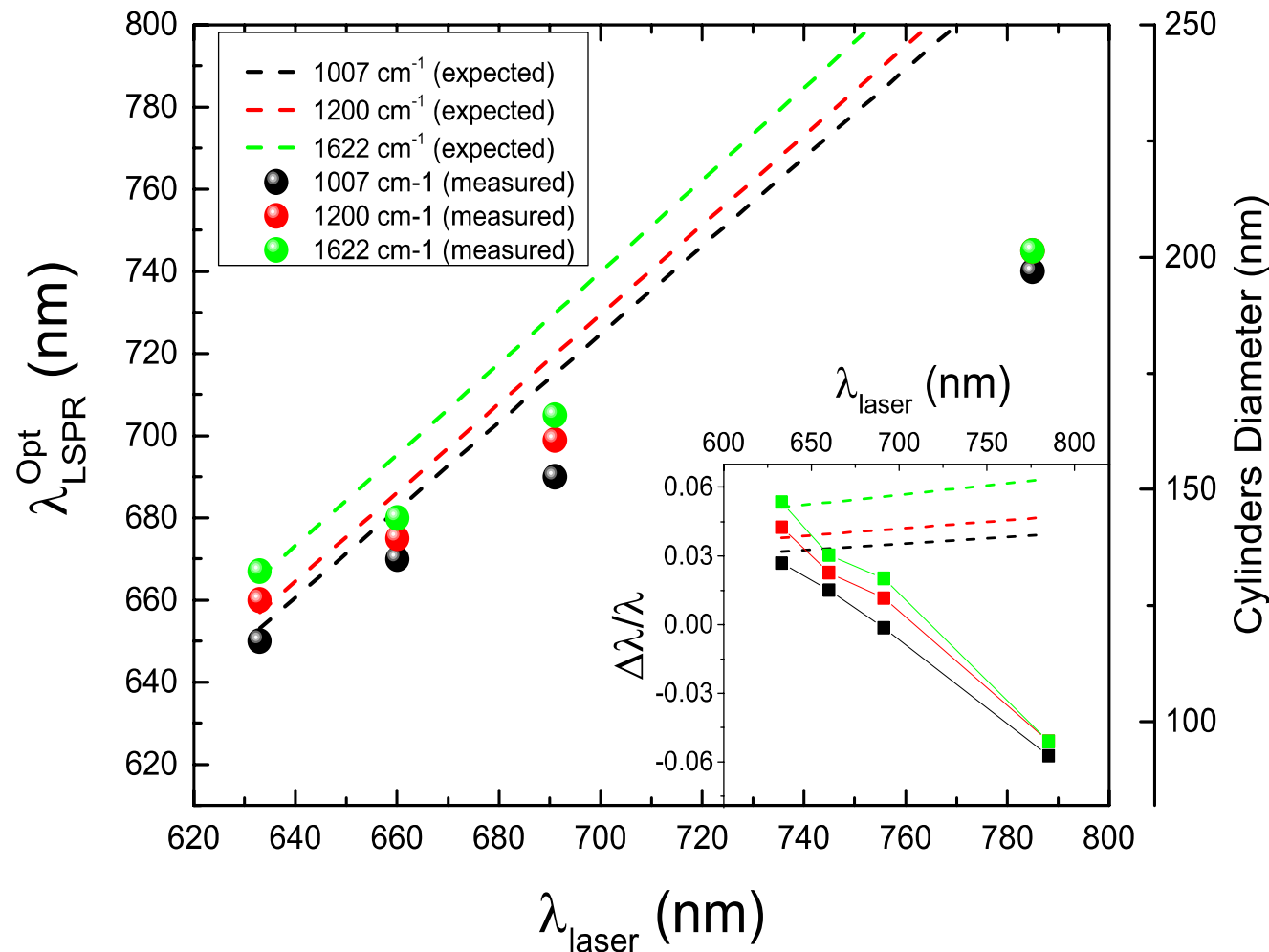
SERS Experiments



SERS Experiments



SERS vs LSPR

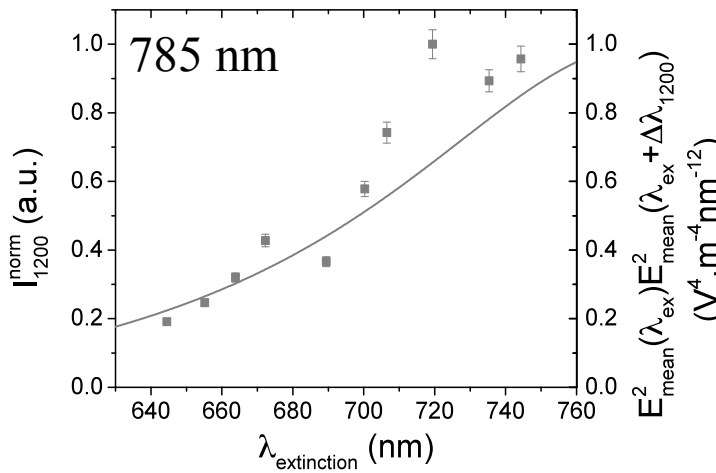
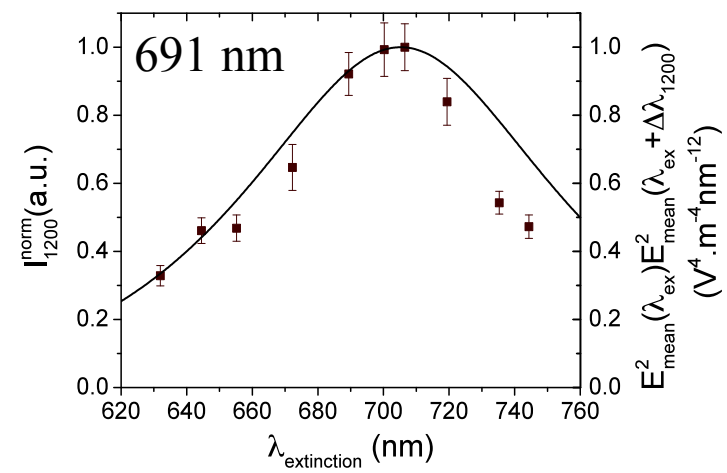
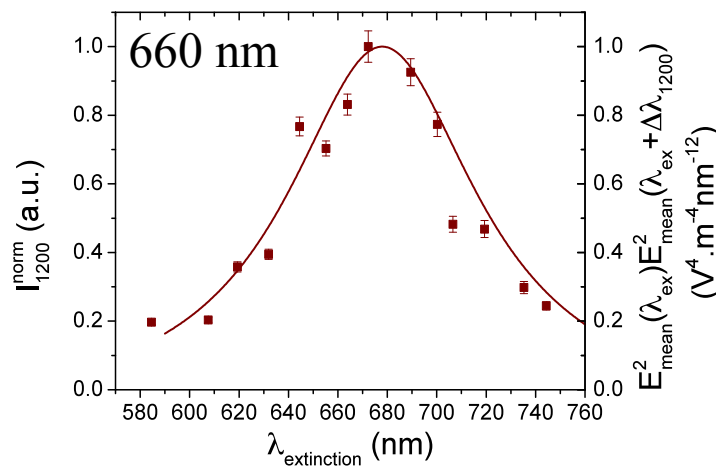
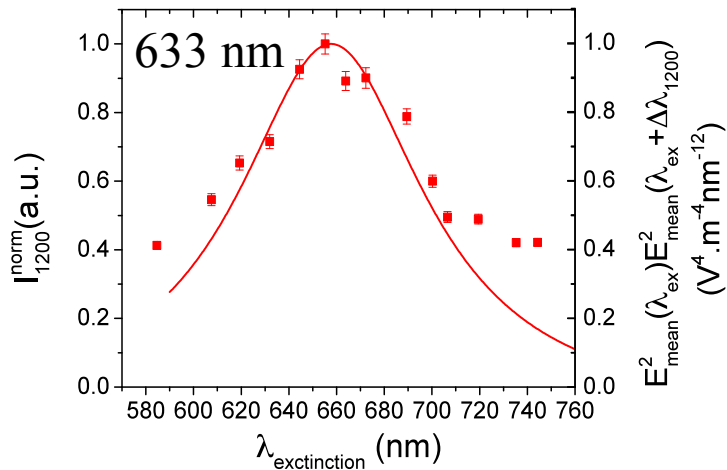


- ➡ Shift between the expected LSPR position and the effective one
- ➡ Near-field / Far-field shift ?

Comparison DDA - Experiments

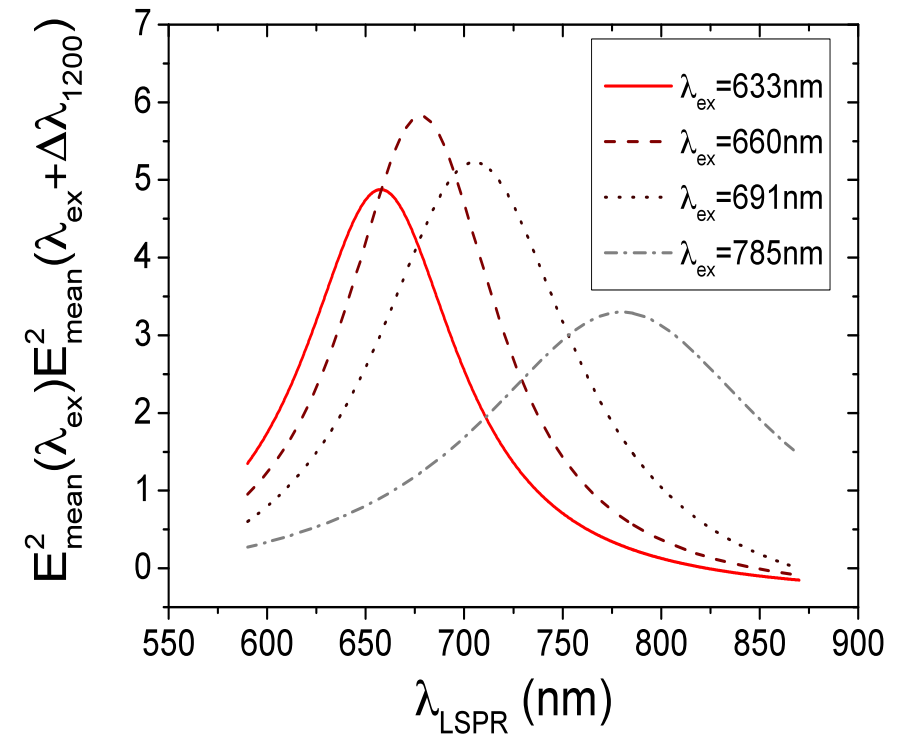
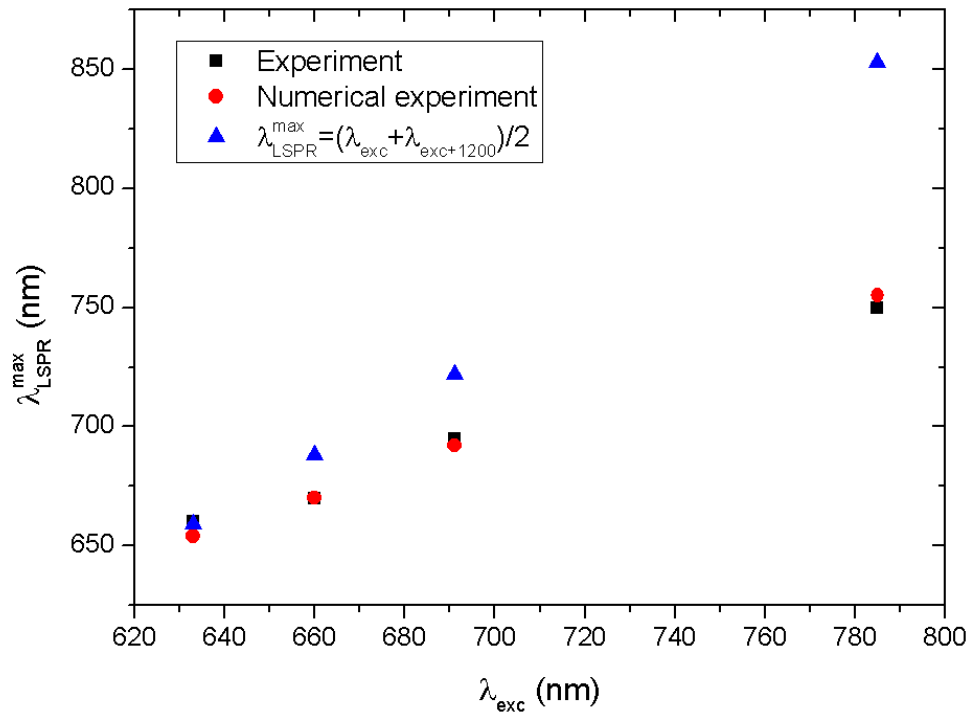
Discrete Dipole Approximation (DDSCAT 7.3)

B. Draine, P. Flatau, JOSA A, 1994, 11(4)1491-1499



⇒ Good agreement between DDA calculations and experiments

Comparison DDA - Experiments

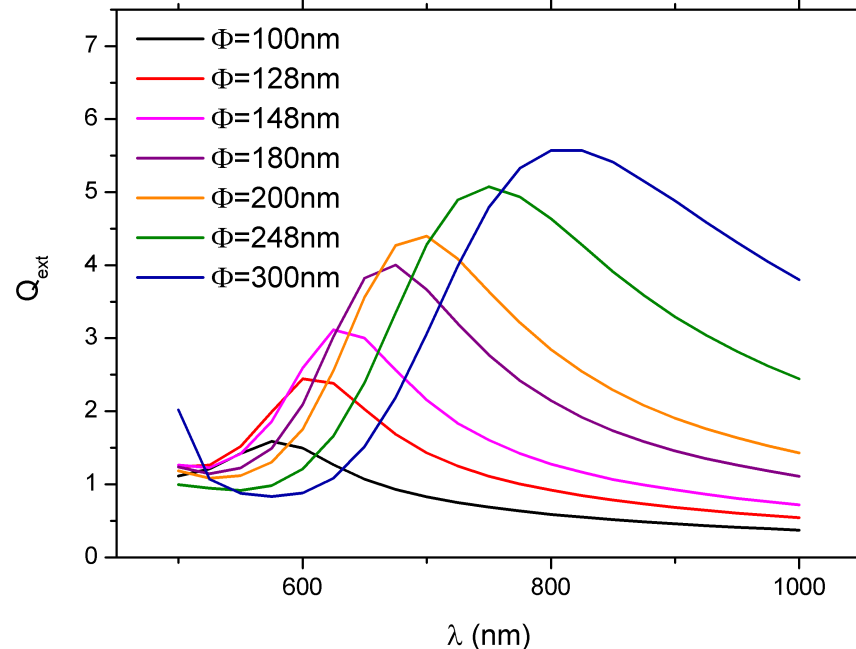


- ⇒ Observation of the shift between the expected and the observed LSPR
- ⇒ Change in the relative intensity of the enhancement

Near-field/Far-field discrepancy

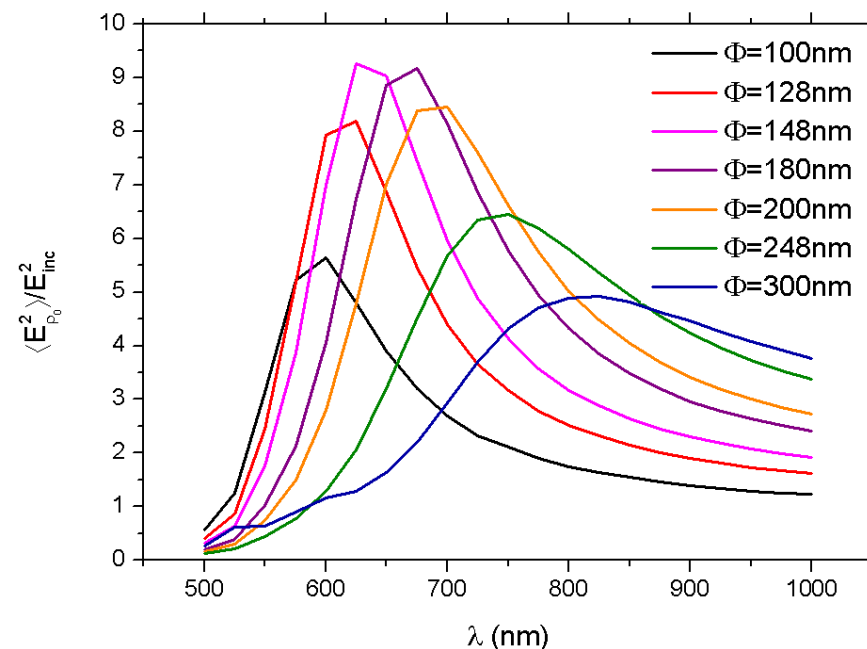
LSPR

Far field measurement



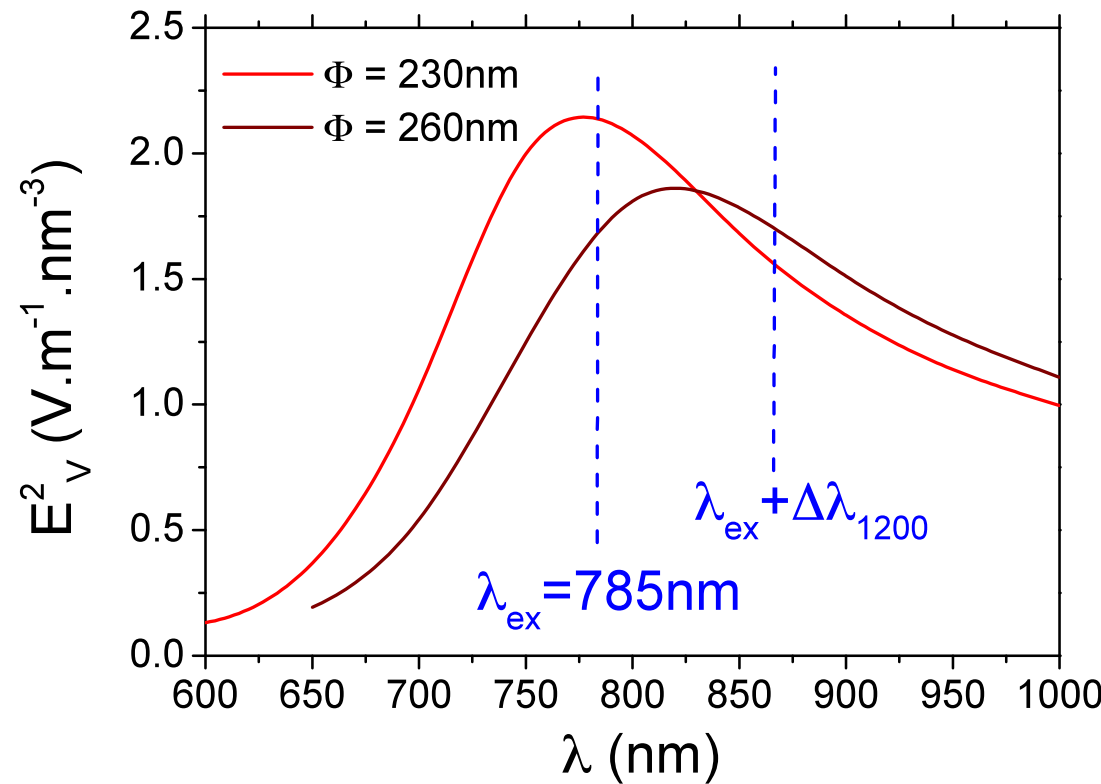
SERS

Near field measurement



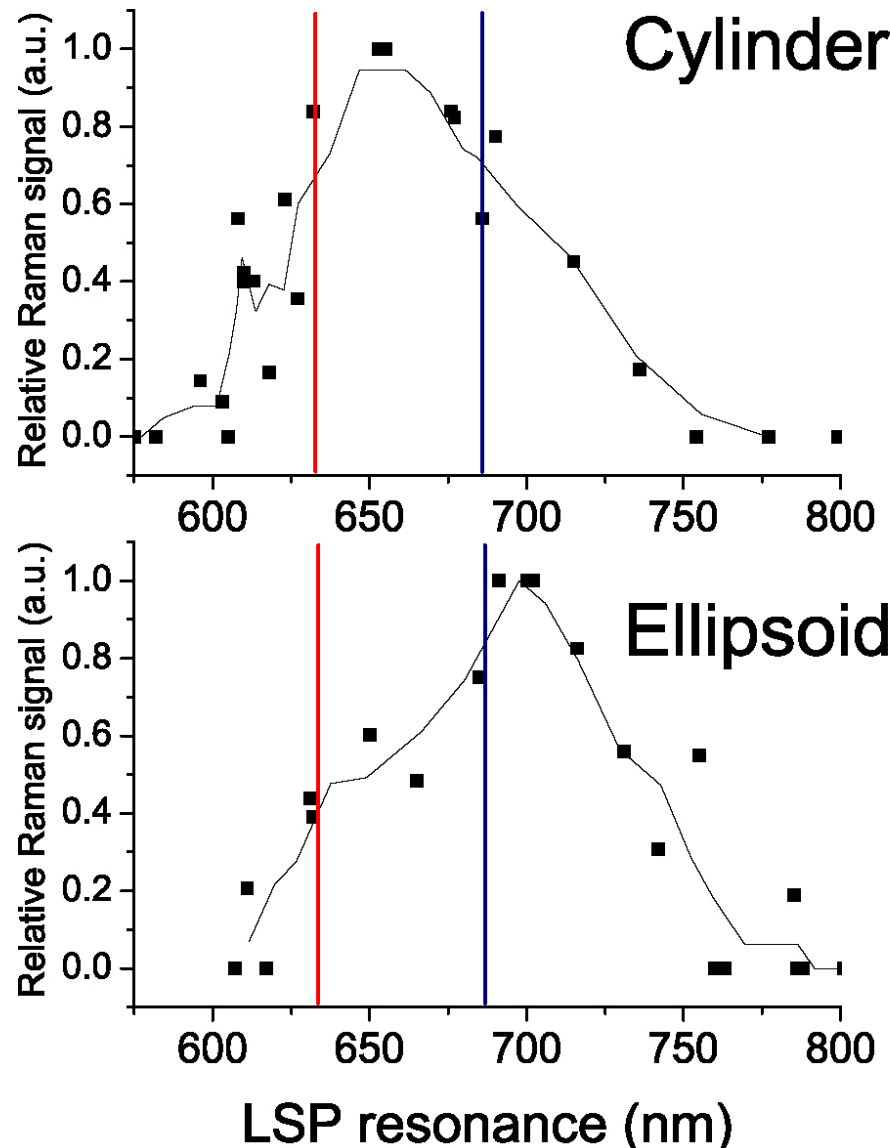
➡ Broadening and decrease of the intensity of the near-field enhancement

Near-field/Far-field discrepancy



⇒ Best SERS enhancement for a lower diameter and thus for a blueshifted LSPR

SERS vs LSPR



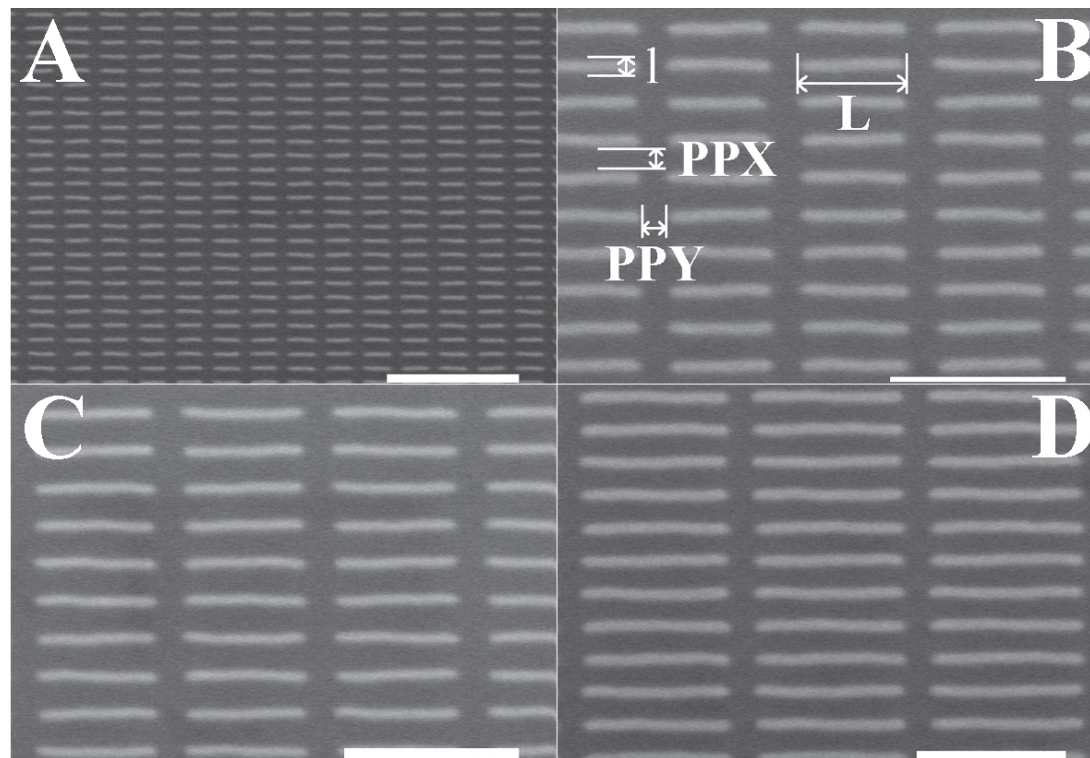
Nanocylinders : $50 \text{ nm} < \text{diameter} < 200 \text{ nm}$
Nano-ellipses : $50 \text{ nm} < \text{major axis} < 200 \text{ nm}$

Excitation Wavelength
 $\lambda_{\text{exc}} = 632.8 \text{ nm}$
BPE Raman mode: 1200 cm^{-1}
 $\lambda_R = 685 \text{ nm}$

$$G_{\text{SERS}} = |f(\lambda_{\text{exc}}) \cdot f(\lambda_R)|^2$$

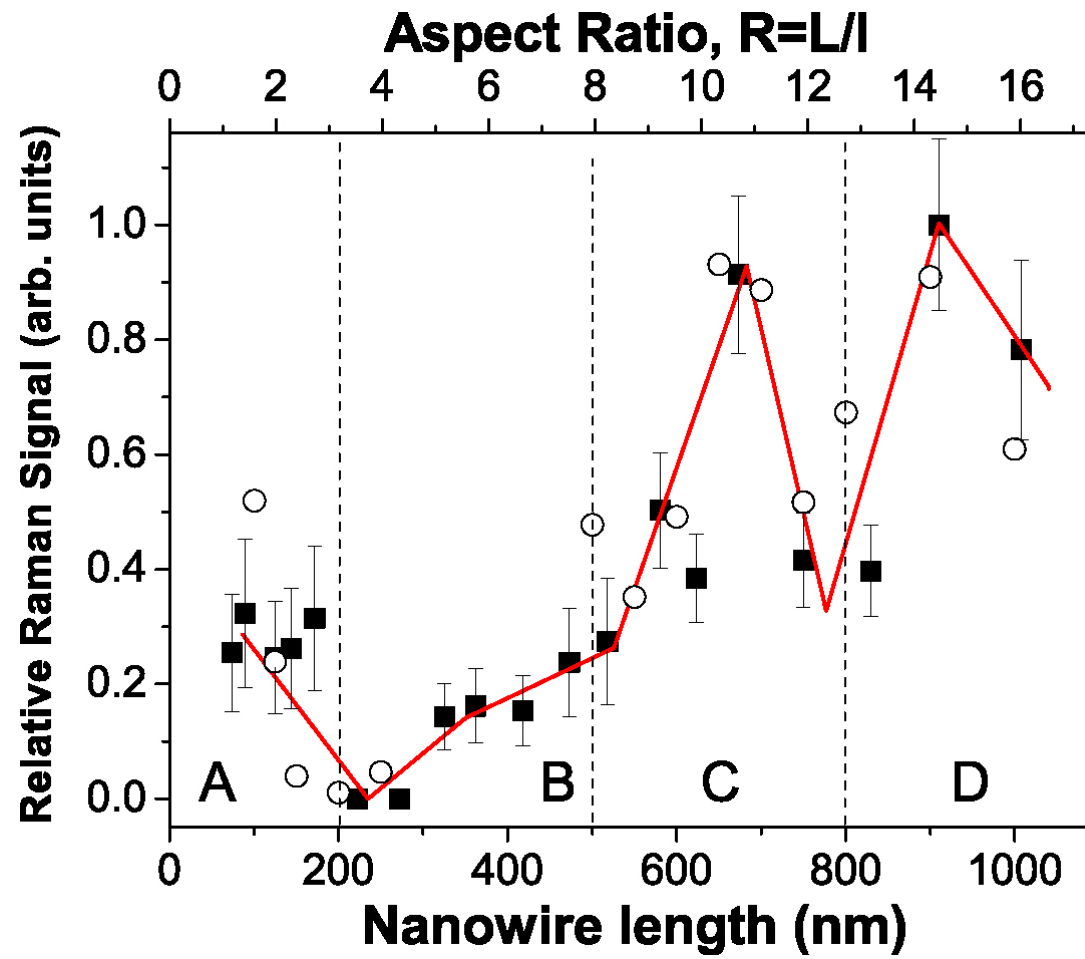
$$G_{\text{SERS Max}} \Rightarrow \lambda_{\text{exc}} < \lambda_{\text{LSPR}} < \lambda_R ?$$

Gold Nanowires



L = from 50 nm to 1000 nm, l = 60 nm, height = 50 nm, PPX = PPY = 200 nm

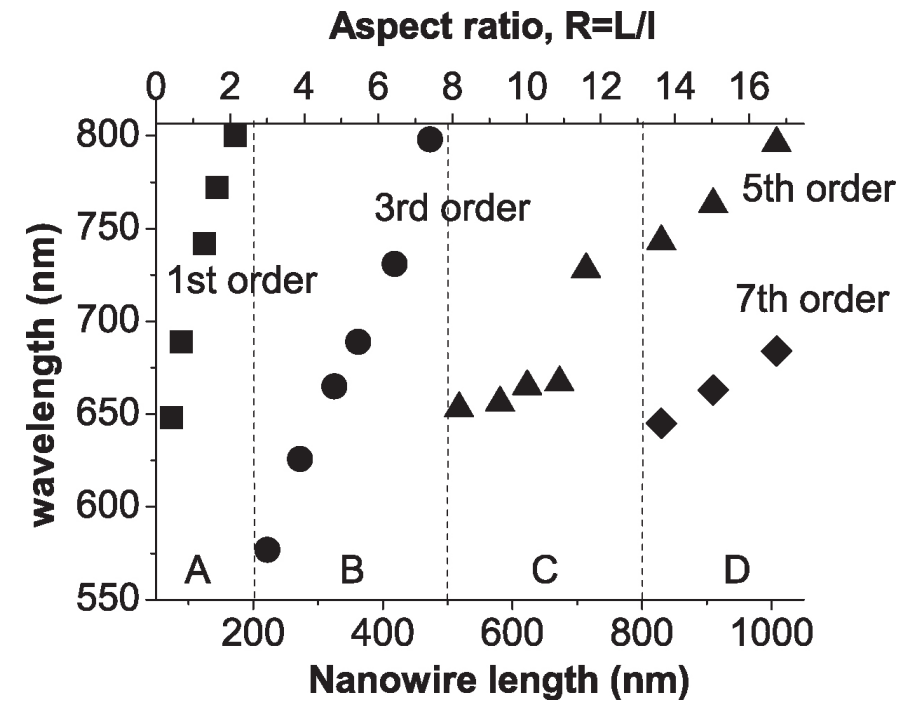
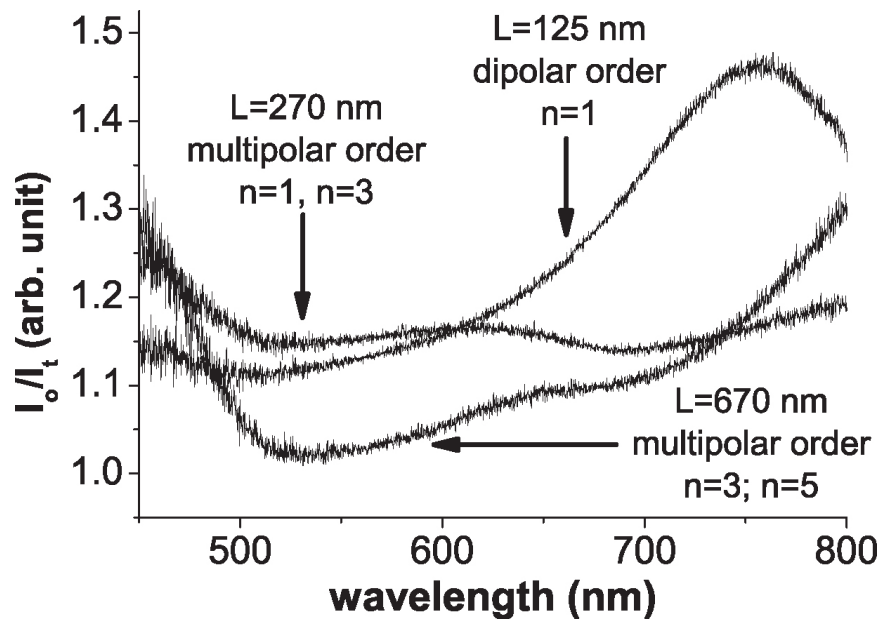
Gold Nanowires : SERS



➡ Raman enhancement maximum for one optimum length

(L. Billot *et al.*, CPL 422, 303, 2006)

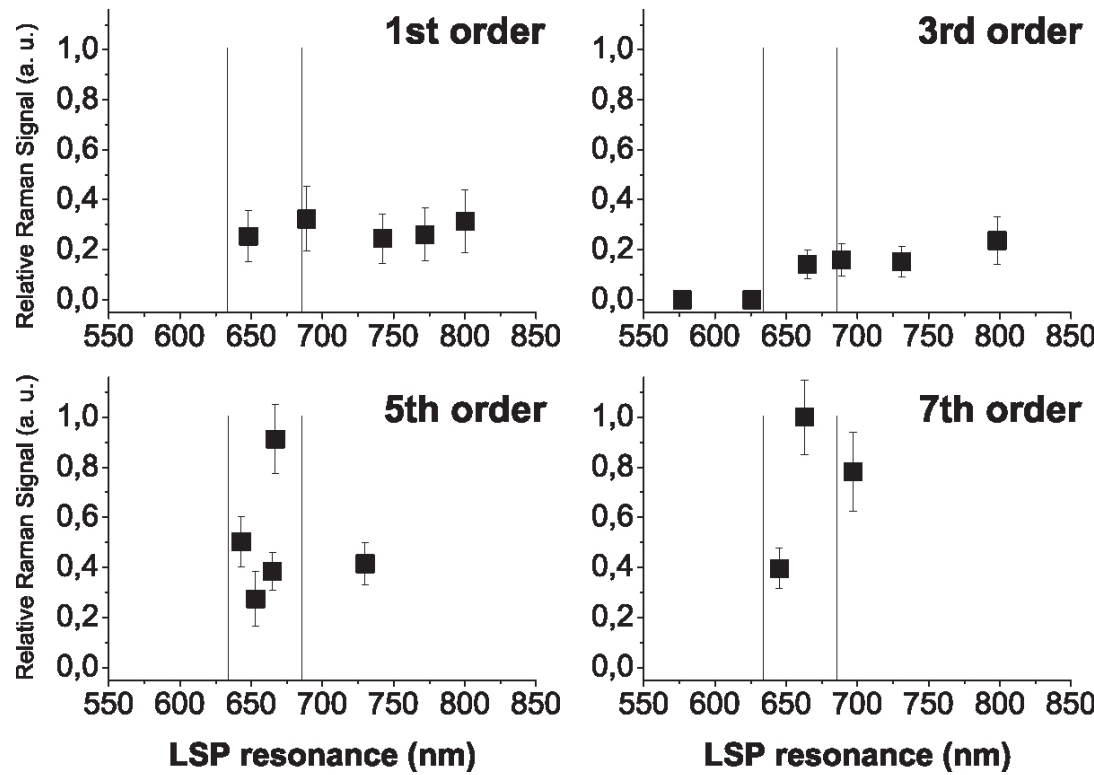
Gold Nanowires : LSPR



⇒ Observation of odd multipolar LSPR

(G. Schider *et al.*, PRB 68, 155427, 2003)

Gold Nanowires : LSPR



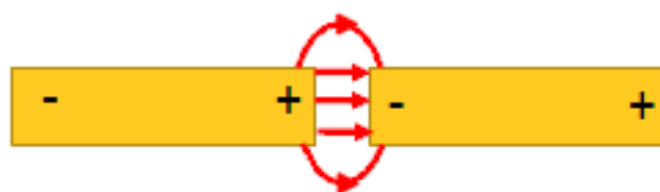
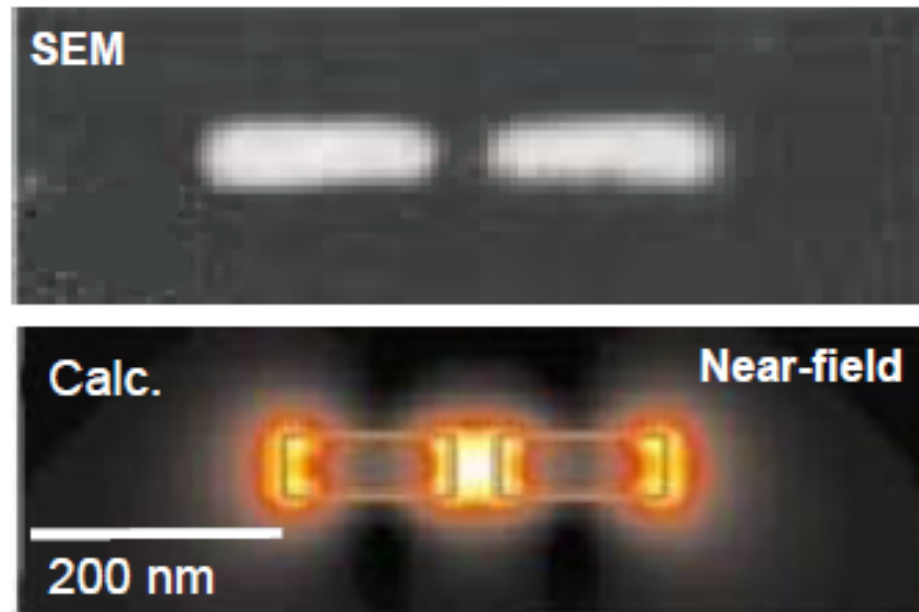
- Best enhancement for LSPR close to 675 nm, $\approx \lambda_R$
- Some multipolar LSPR have better enhancement than dipolar LSPR

LSPR rules

λ_{Exc}	633	660	785	633, 676	514, 532 633
λ_{LSPR} rules	$= (\lambda_0 + \lambda_R)/2$	$\approx \lambda_0$	$< \lambda_0$	$\approx \lambda_R$	$\lambda_0 < \lambda_{LSPR} < \lambda_R$

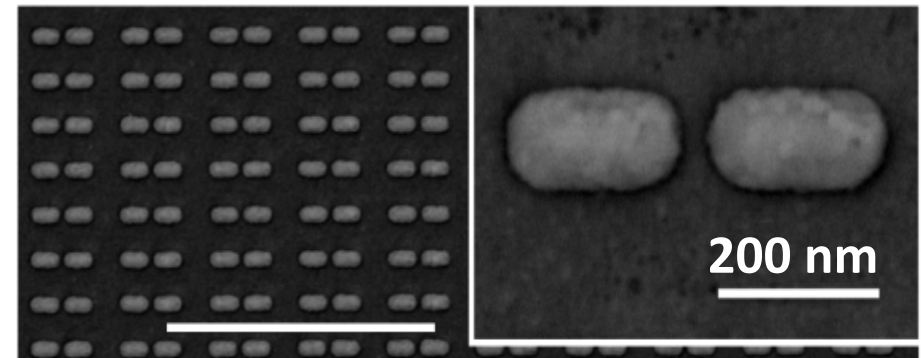
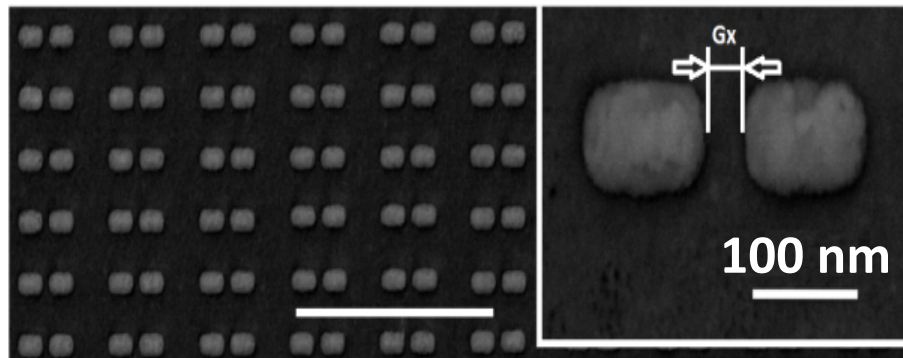
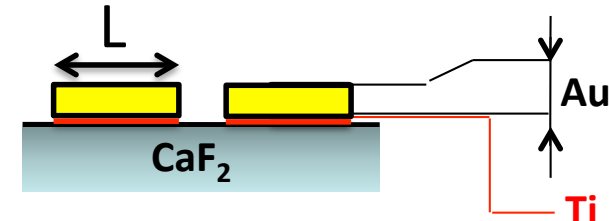
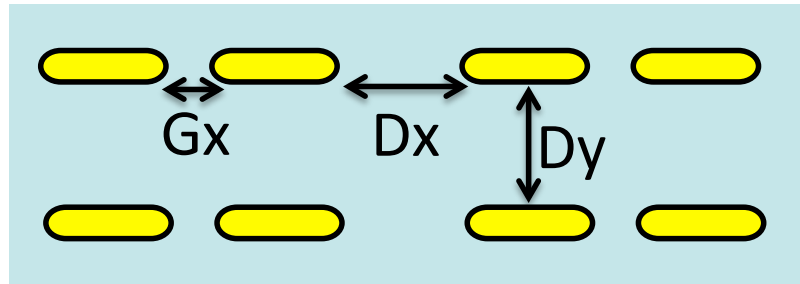
⇒ The LSPR rules depend on the shape of the nanostructures
and on the excitation wavelength

Electromagnetic Coupling



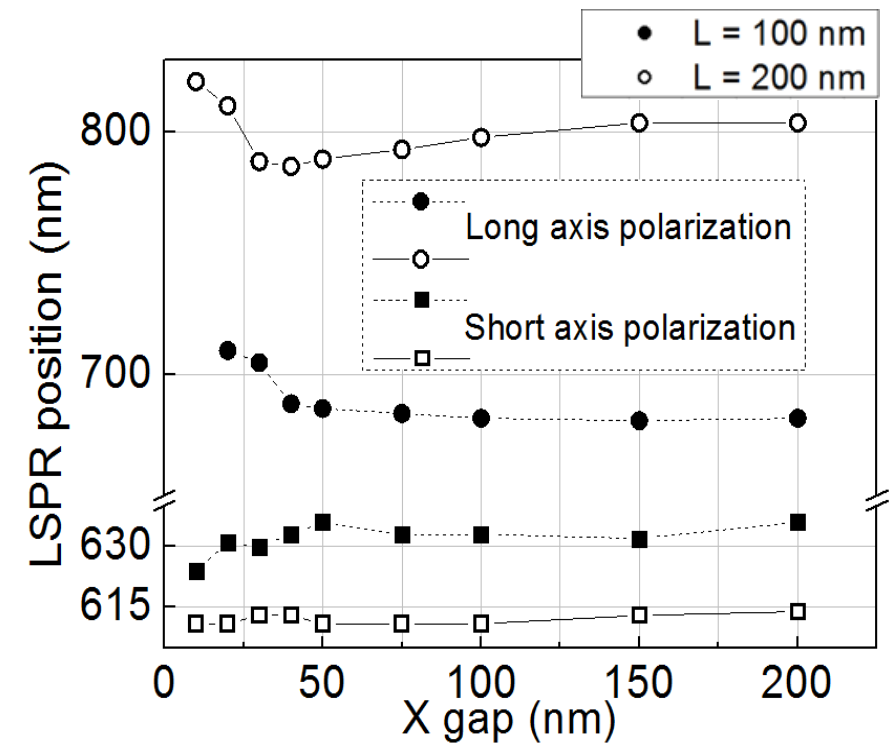
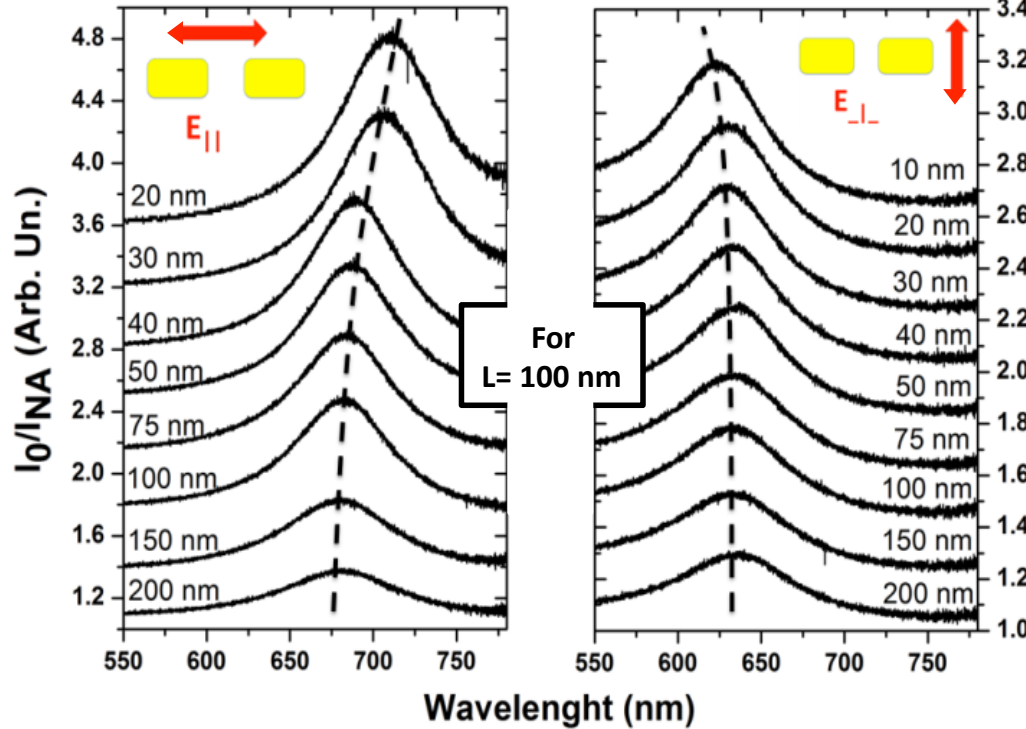
**Systematic study to measure the consequences of coupling
on LSPR and on SERS**

Electromagnetic Coupling



G_x (nm)	Length L (nm)	Height=Width (nm)	$D_y=D_y$
10,20,30,40,50, 75,100,150,200	100	60	200
10,20,30,40,50, 75,00,150,200	200	60	200

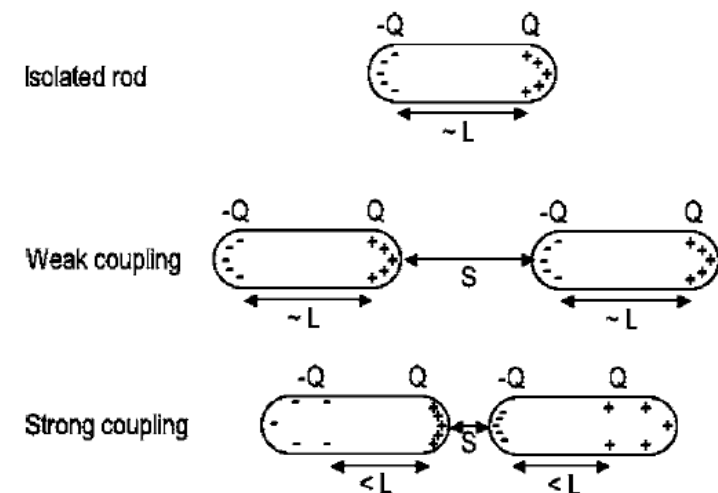
Electromagnetic Coupling: LSPR



$E_{||}$ field polarization = LSPR Redshift

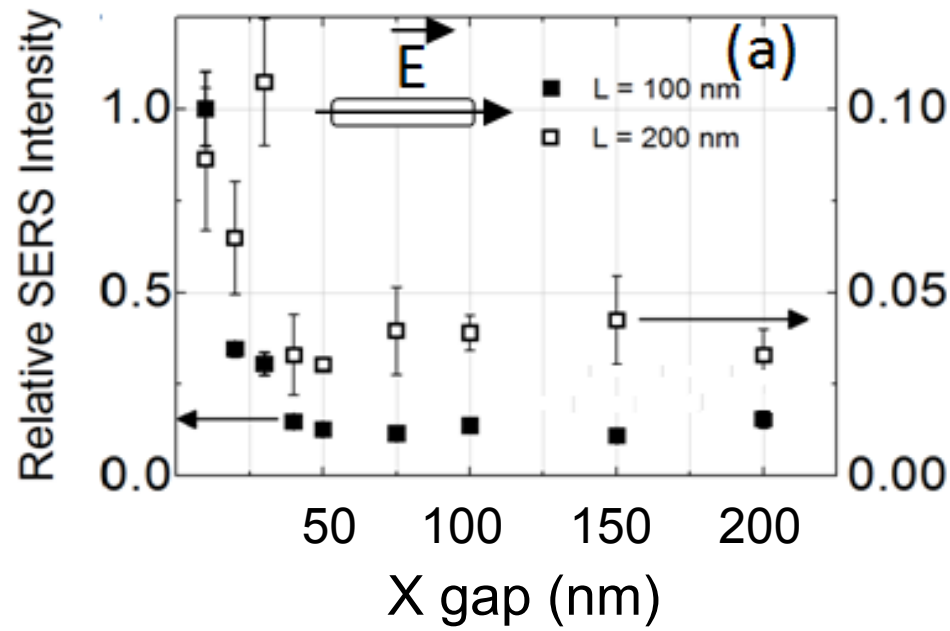
E_{\perp} field polarization = LSPR Blueshift

Typical of a coupling effect

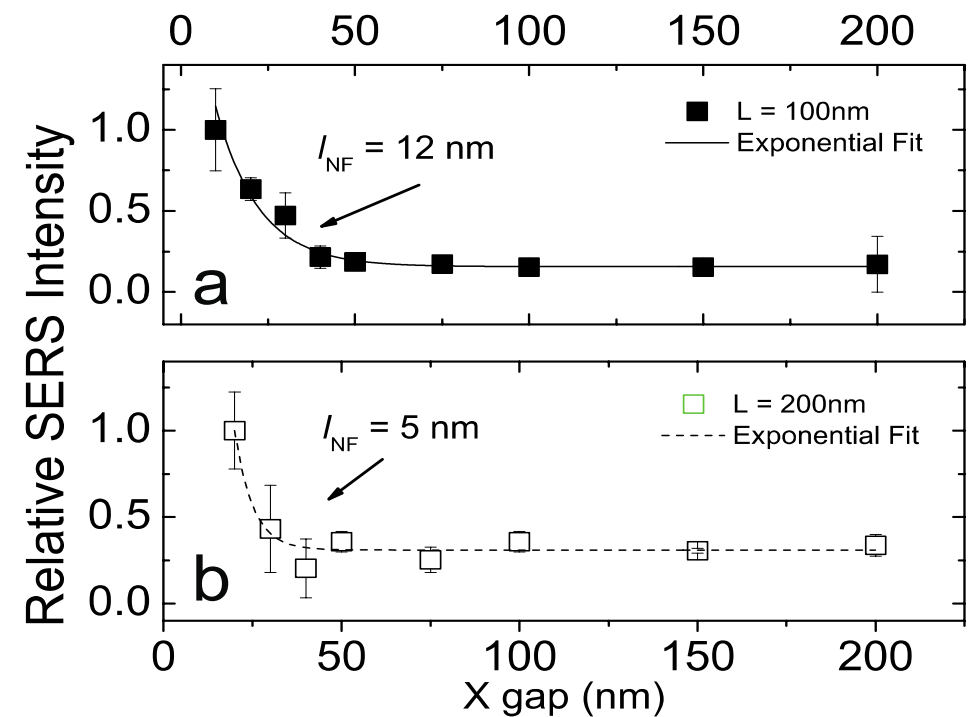


Electromagnetic Coupling: SERS

BPE (10^{-3} M)

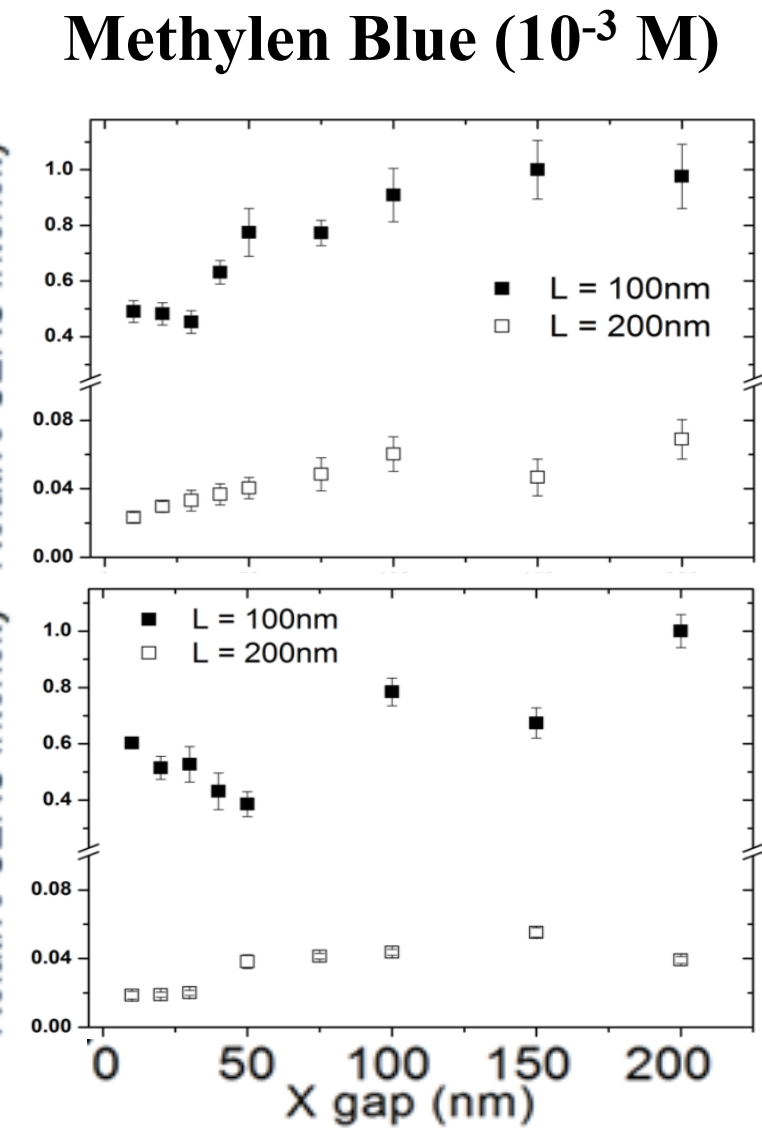
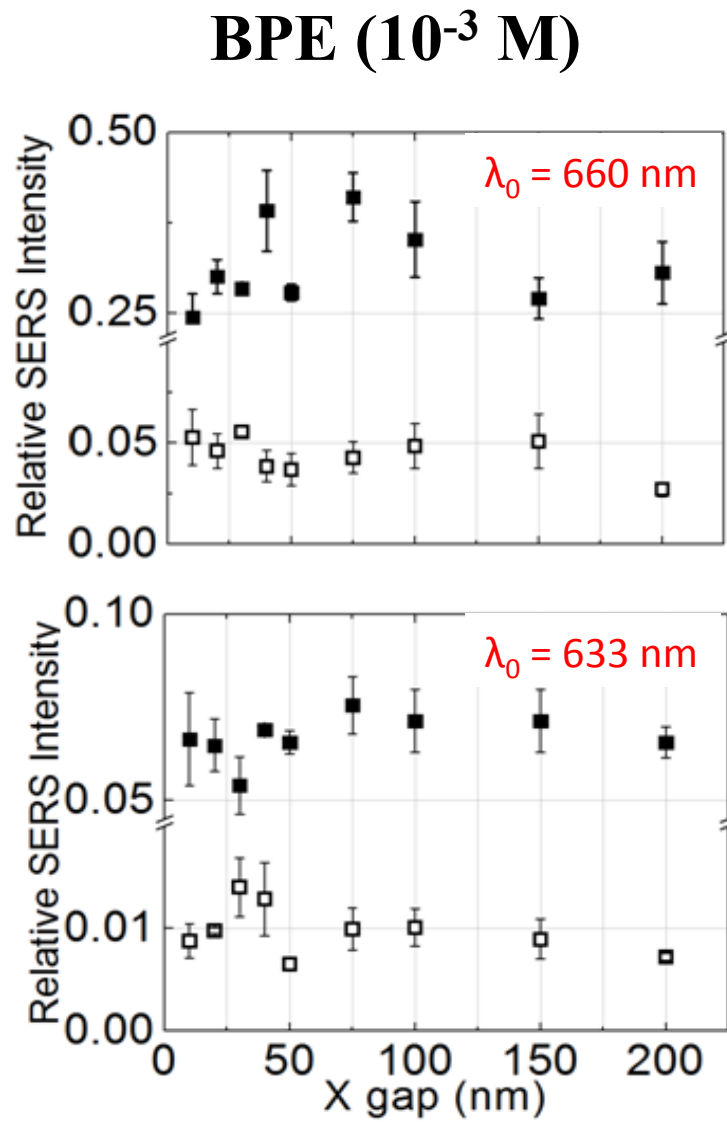


Methylen Blue (10^{-3} M)



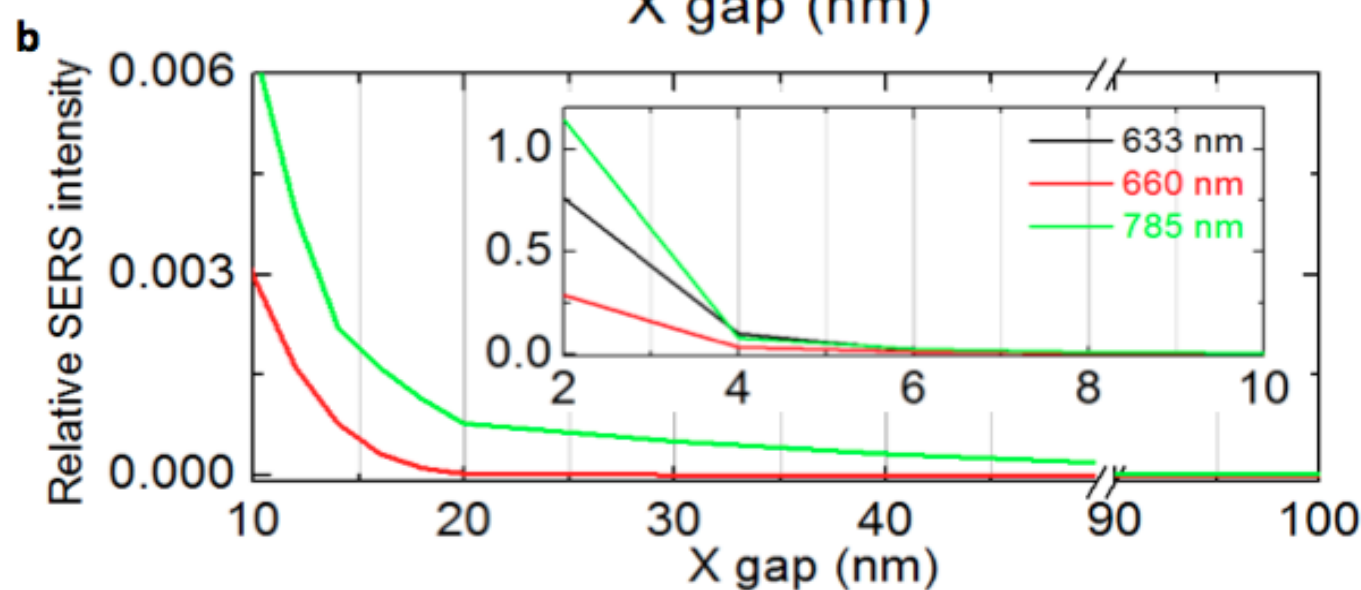
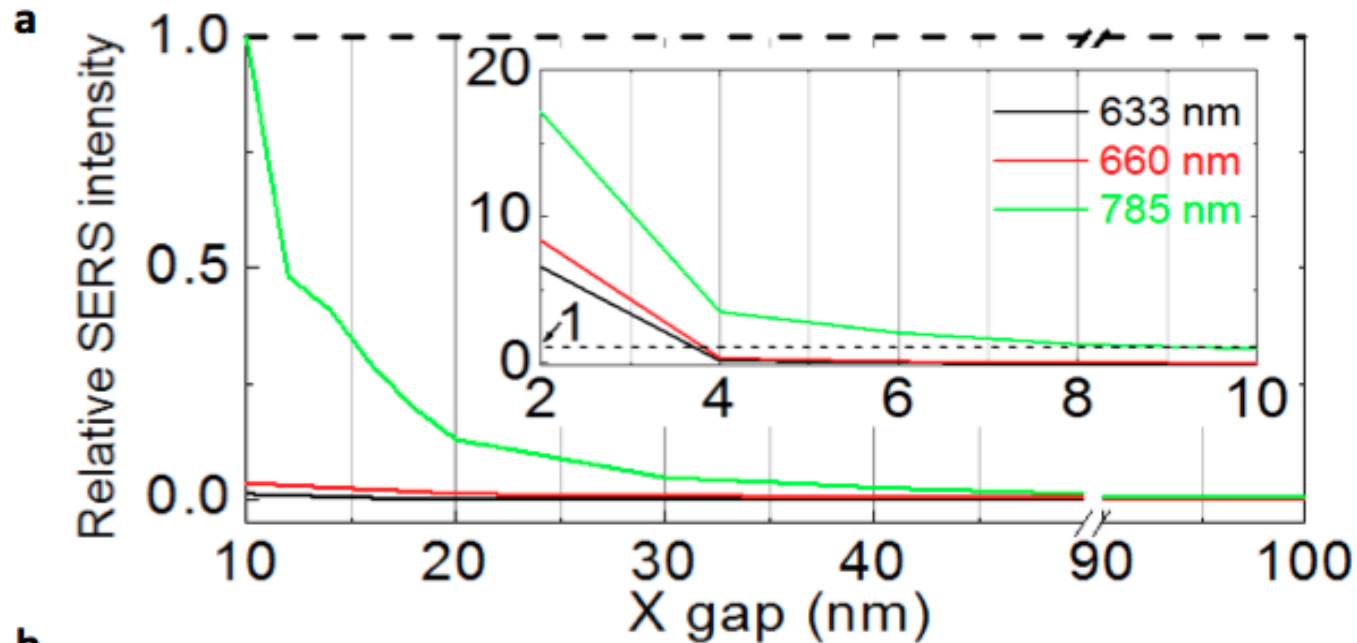
→ Coupling for a lower gap and lower SERS intensity for $L=200$ nm

Electromagnetic Coupling: SERS



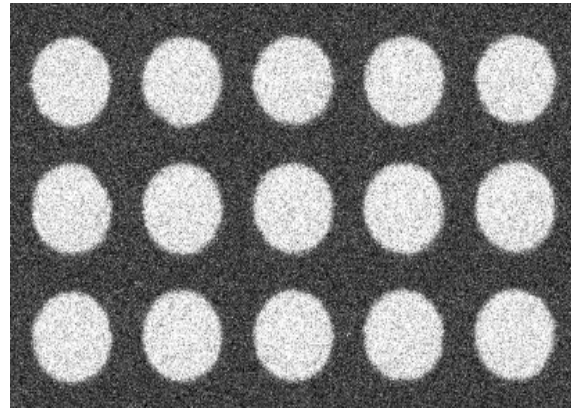
→ No coupling for excitation wavelength at 633 and 660 nm

Electromagnetic Coupling: simulation

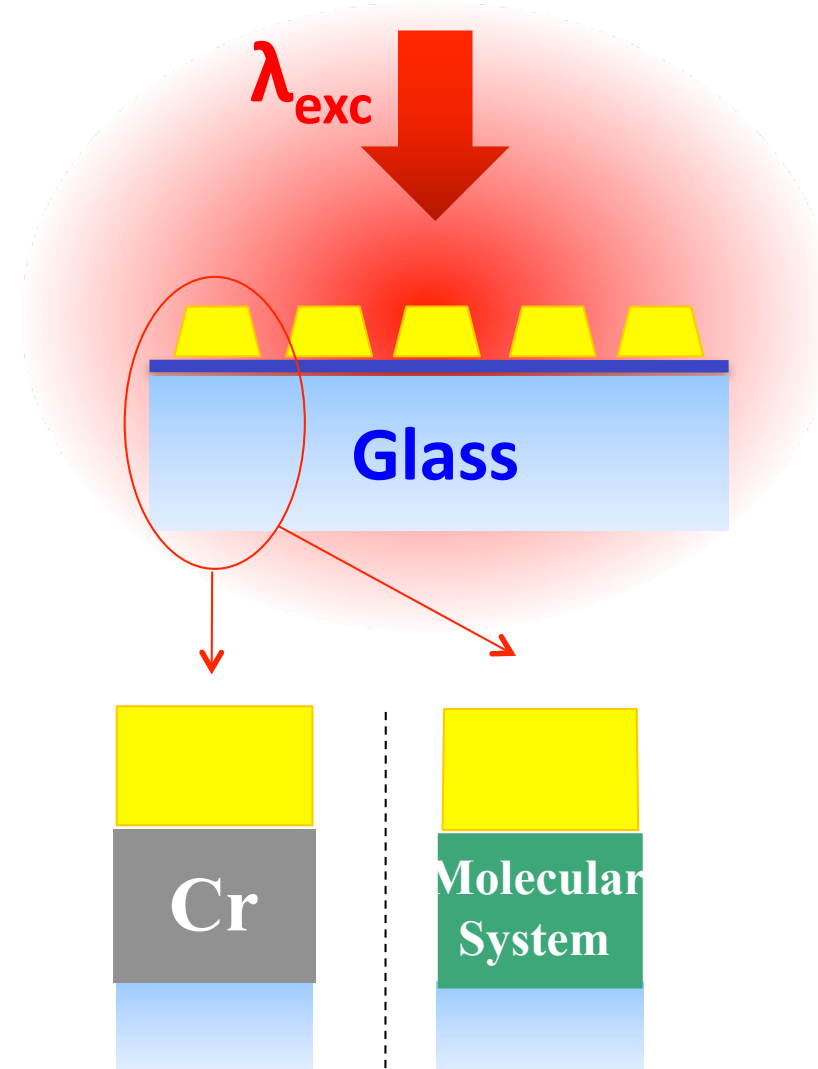


➡ Confinement of few nm for L=200 nm

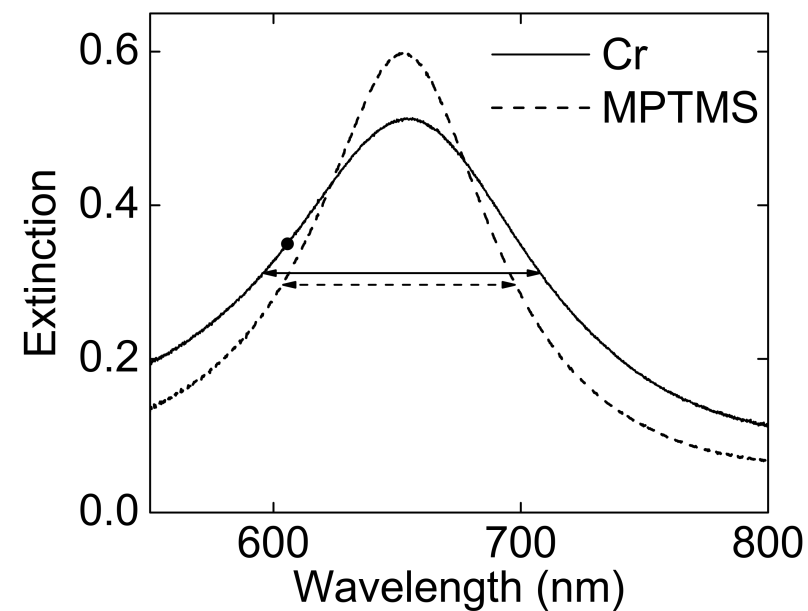
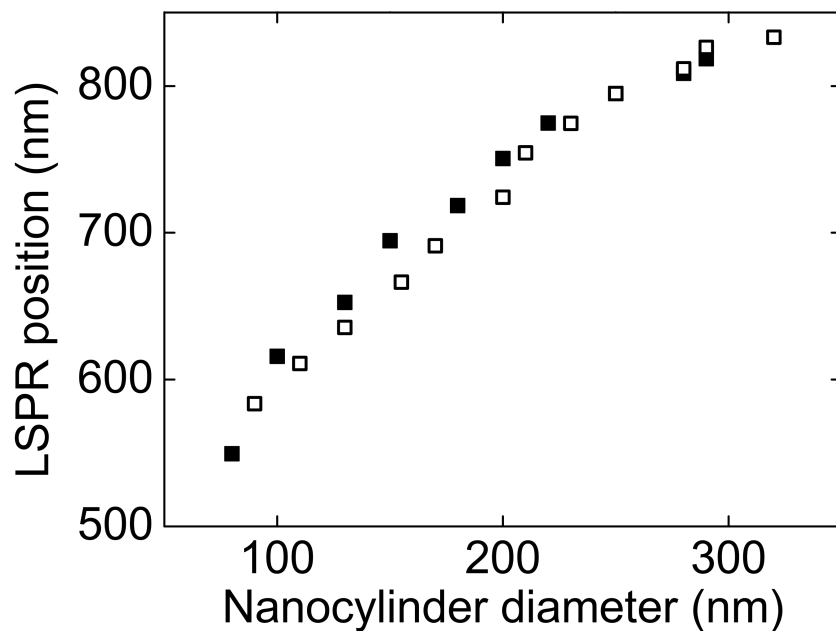
Adhesion layer



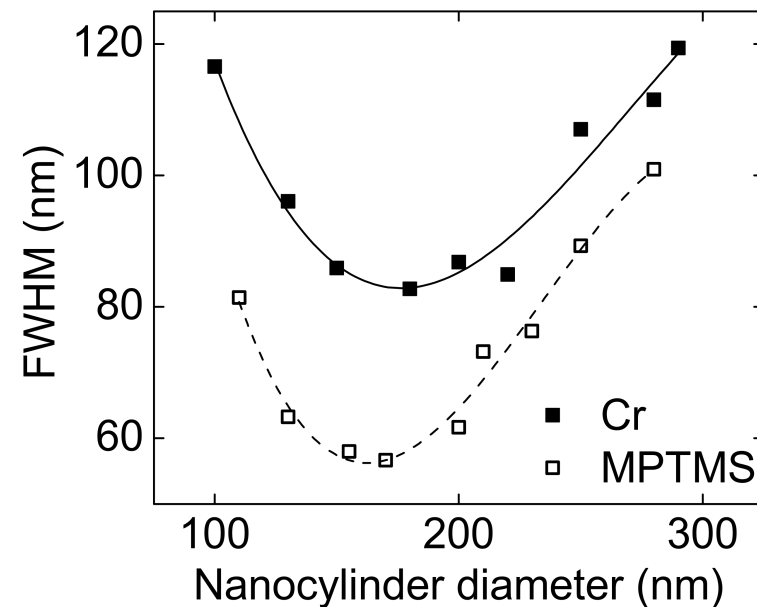
**Adhesion layer
between glass and gold
⇒ Cr or MPTMS**



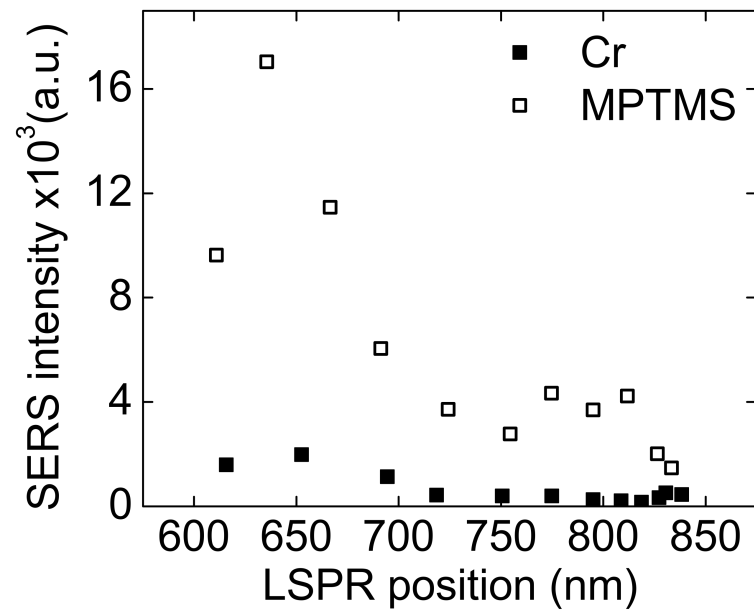
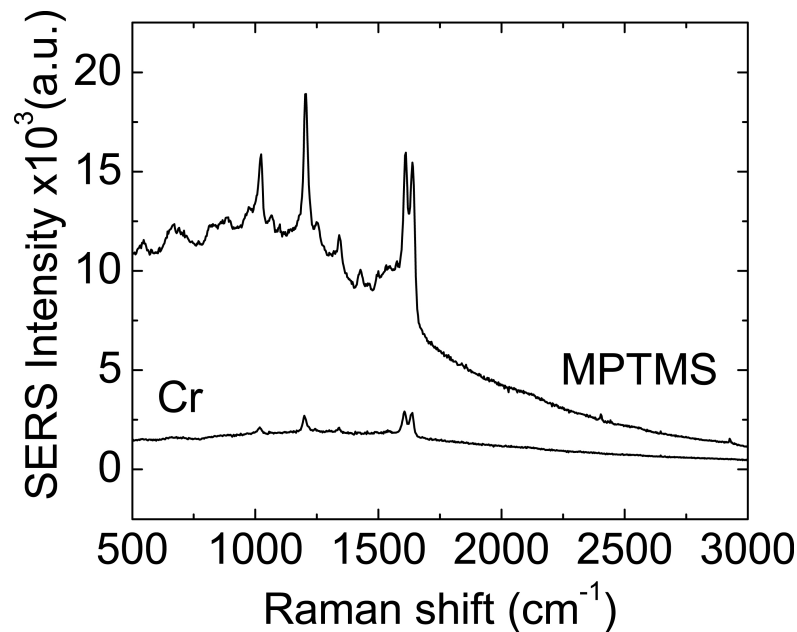
Adhesion layer: LSPR



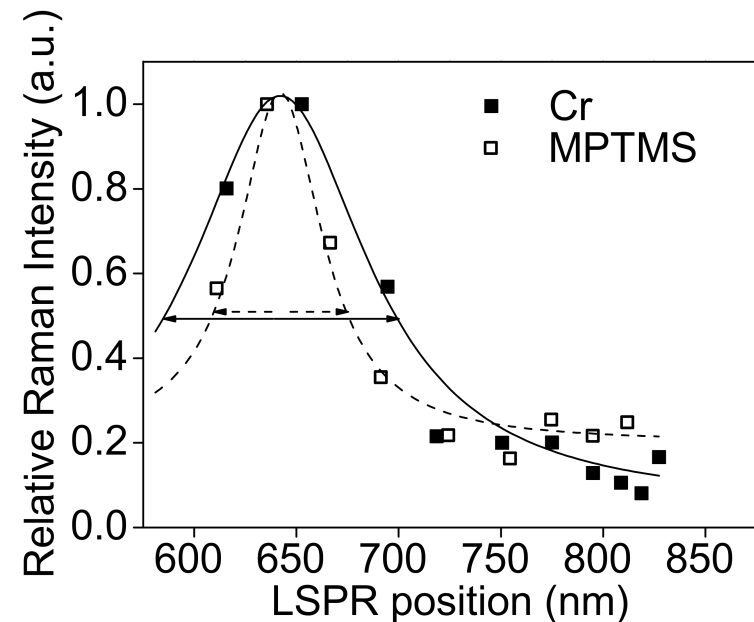
- No modification of the LSPR position
- Improvement of the Q factor of the LSPR



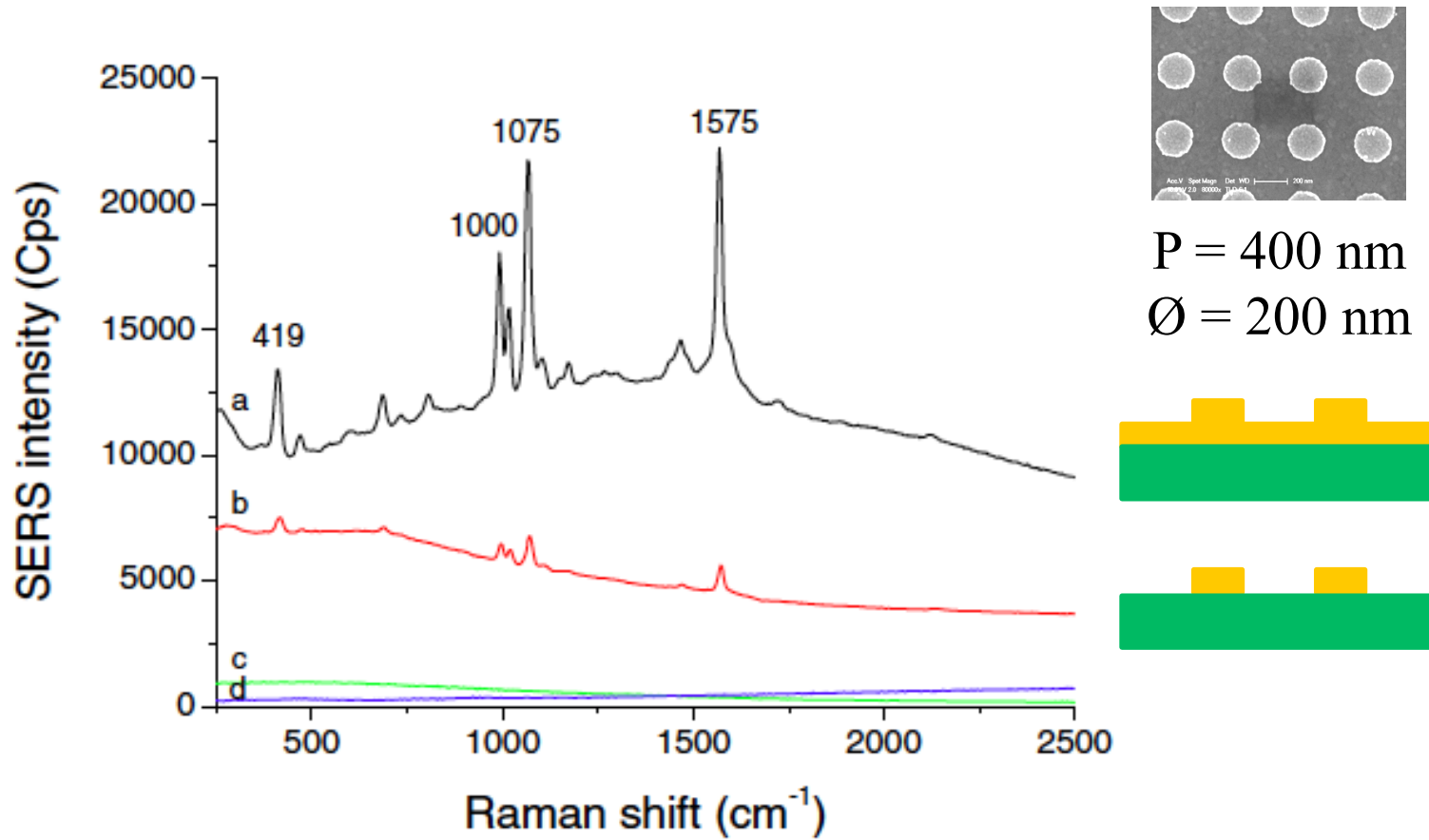
Adhesion layer: SERS



⇒ Improvement of the
SERS signal
by one order of
magnitude



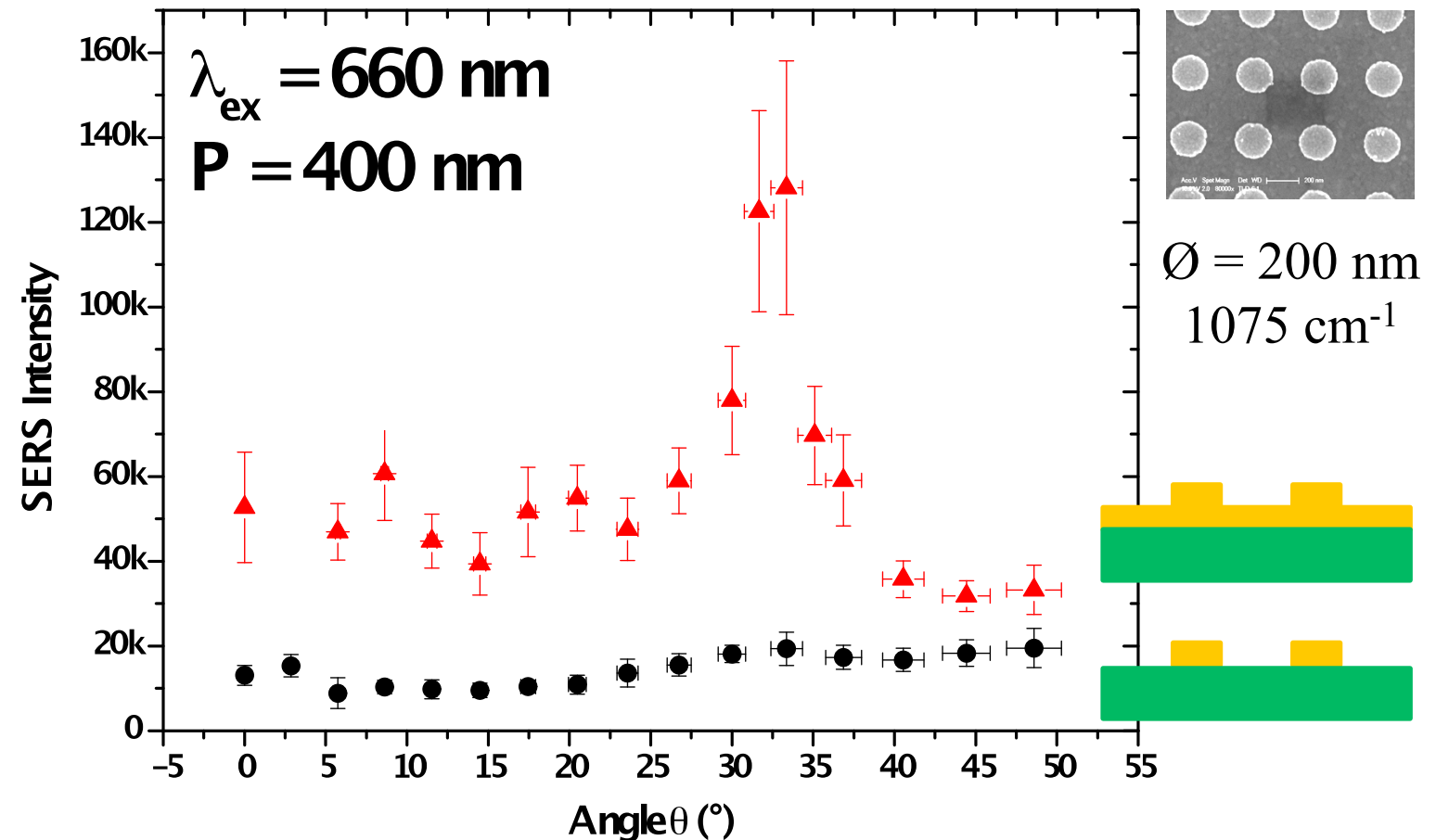
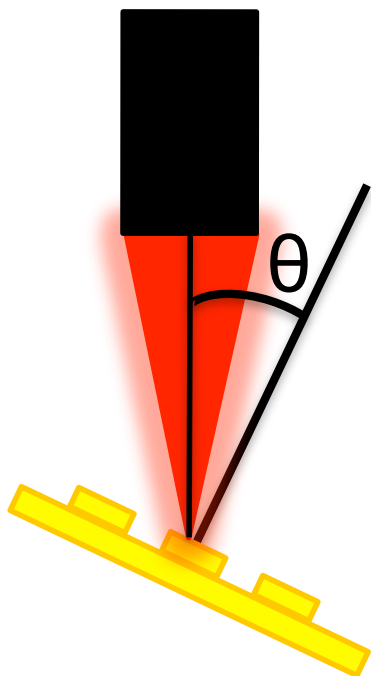
Influence of the substrate : SERS



→ SERS intensity one order of magnitude higher
with gold film

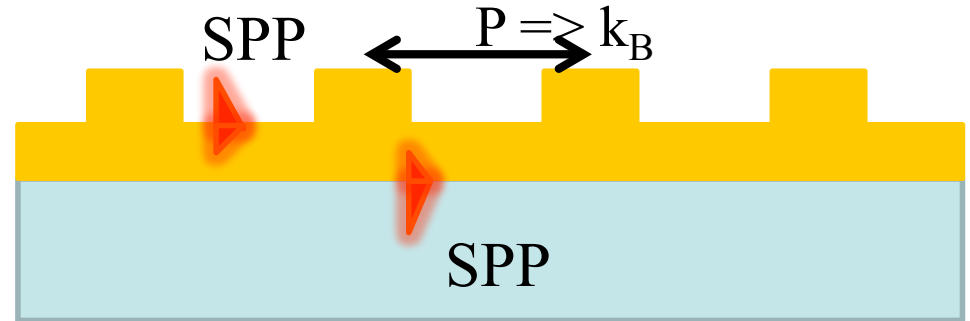
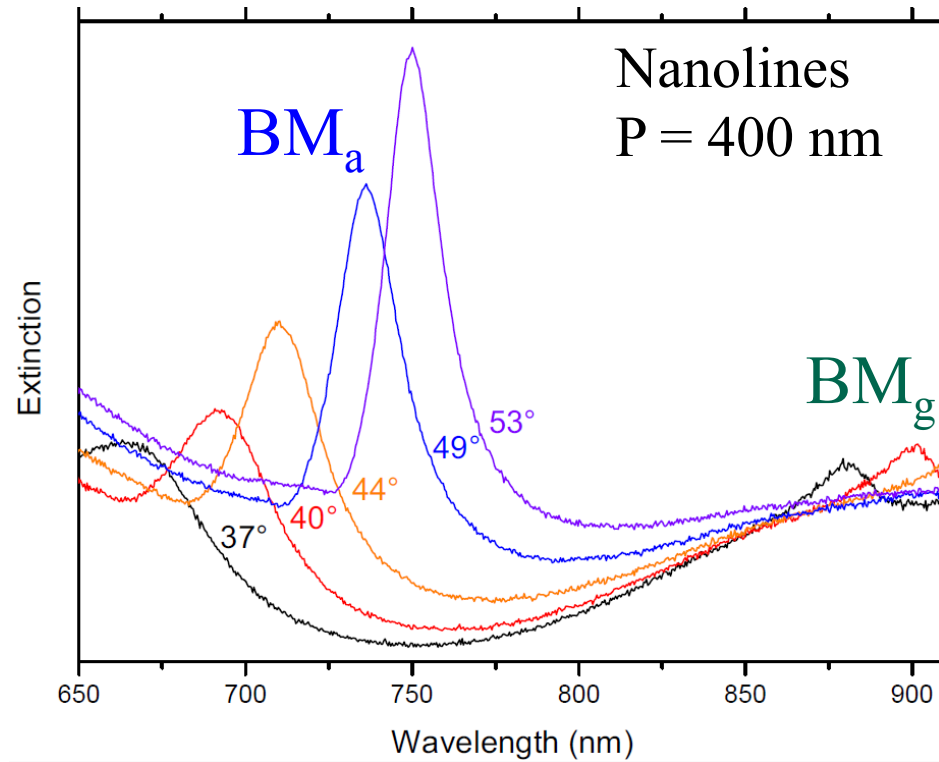
Influence of the substrate : SERS

10x Obj.
N.A. = 0.25



Gold film => angular dependence
Without gold film => no dependence

Influence of the substrate : Plasmon



$$\begin{aligned} k_{BM} &= k_{spp} \pm k_B \\ &= k_0 \sin \theta \quad \left[\begin{array}{c} \text{Bragg} \\ \text{conditions} \end{array} \right] \end{aligned}$$

$k_{spp}^{a, g}$ Gold/Air or Gold/Glass

⇒ Constructive interferences when $k_{spp} \pm k_B = k_0 \sin \theta$

⇒ Excitation of a Bragg Mode (BM_a and BM_g)

Conclusions

1. Optimization of the gold nanostructure

I. LSPR rules depends on shape and excitation wavelength

- Far field / Near field
- Tip effect

II. Coupling

III. Nanostructure environment

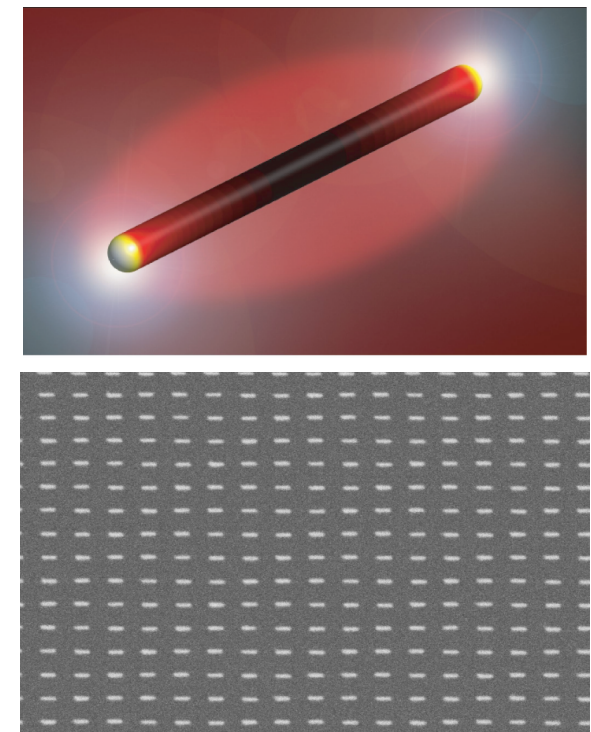
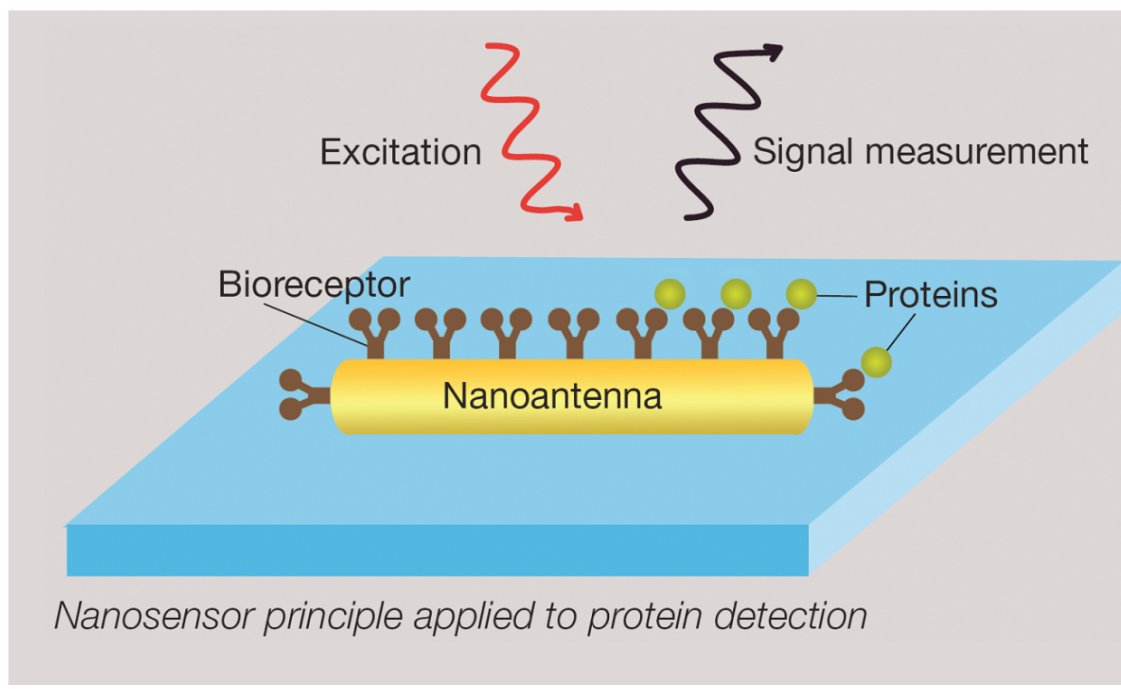
2. Gold nanostructure arrays

➡ Reproducible SERS nanosensor

➡ Sensorchip

SERS sensor

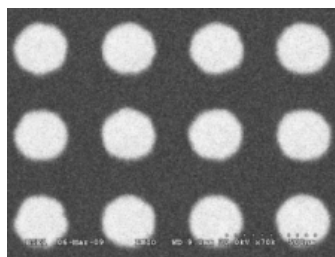
Sensor principle



4 steps approach

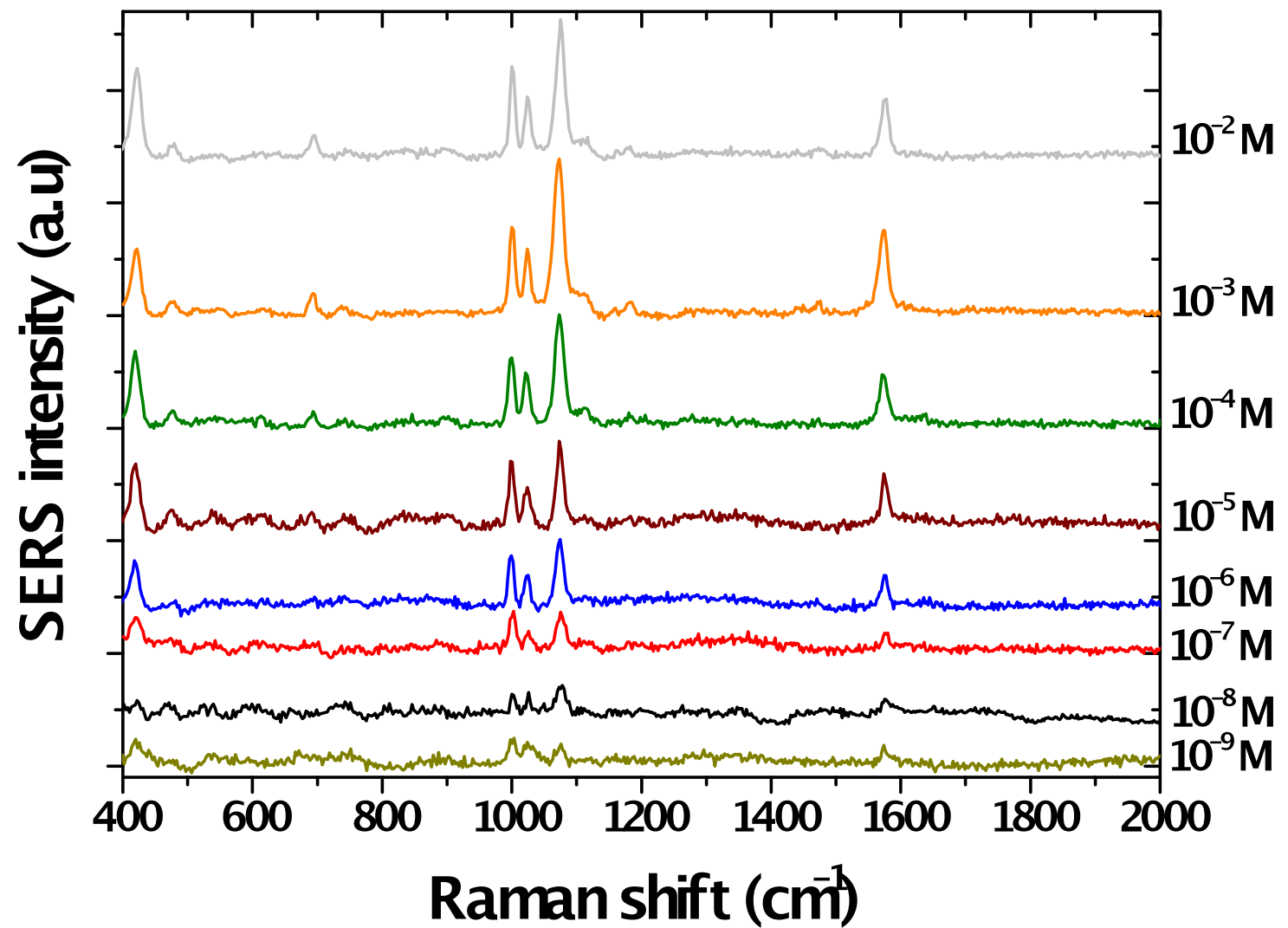
- 1. Raman spectroscopy: **Label Free detection**
- 2. Nanoparticle: **High sensitivity**
- 3. Bioreceptor: **High molecular selectivity**
- 4. Nanoparticle array: **High reproducibility**

Sensor limit of detection



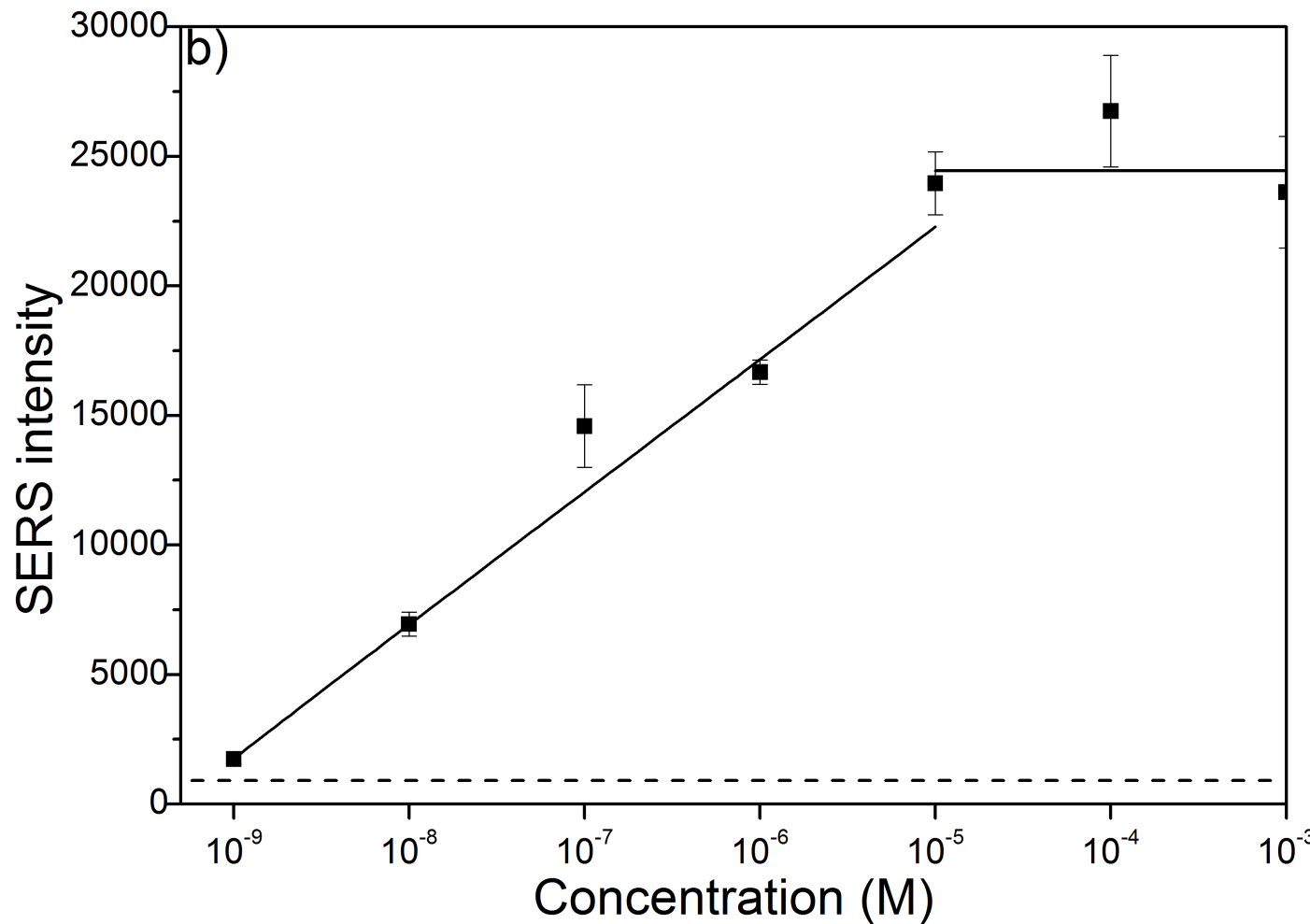
$\varnothing = 190 \text{ nm}$

Benzenethiol
 $\lambda_{\text{exc}} = 785 \text{ nm}$



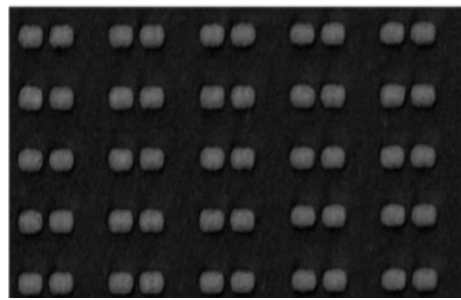
Sensor limit of detection

$\lambda=785\text{nm}$



- ➡ Surface saturation at $10 \mu\text{M/L}$
- ➡ At 785 nm, LOD = 1 nM/L

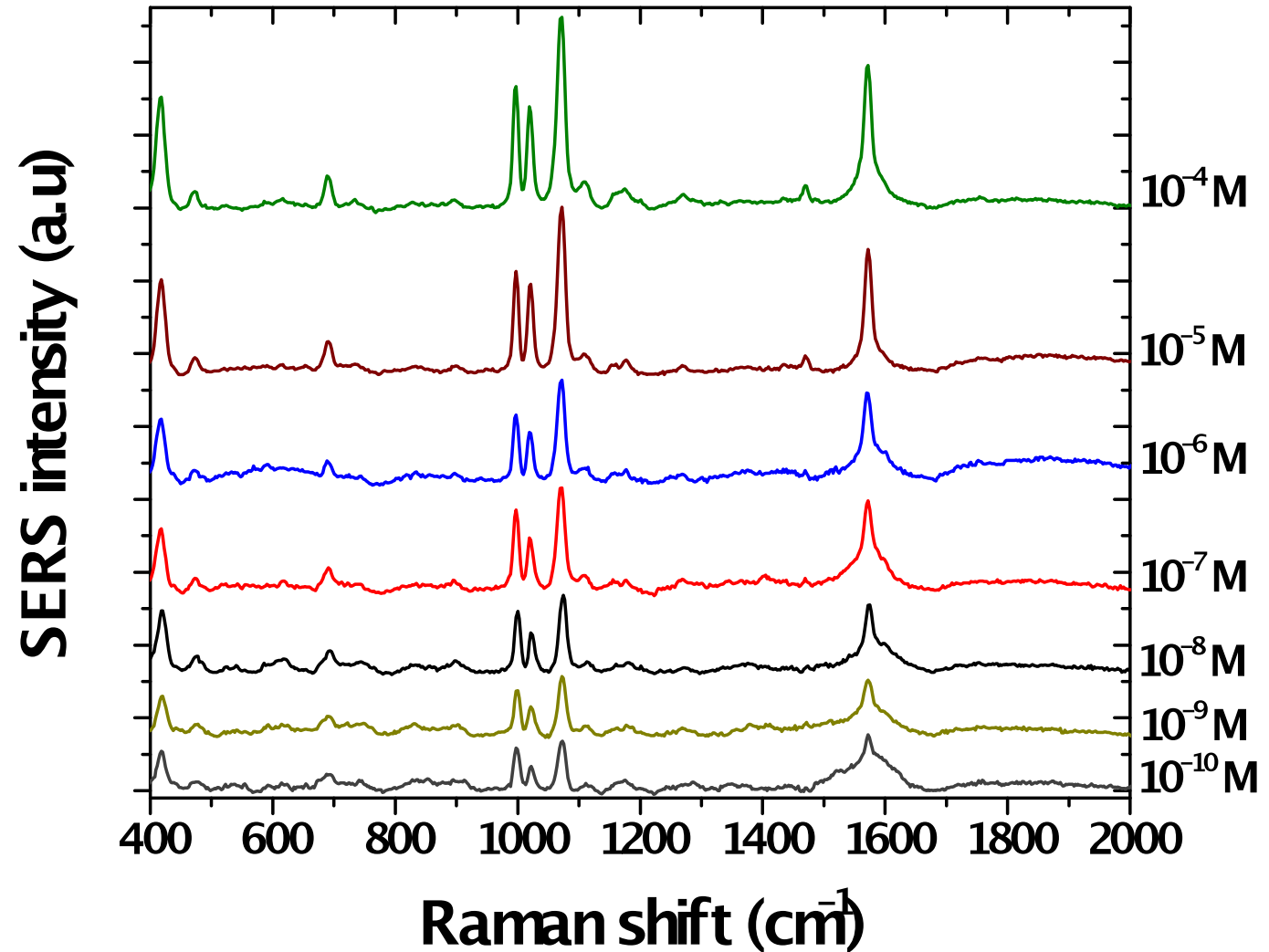
Sensor limit of detection



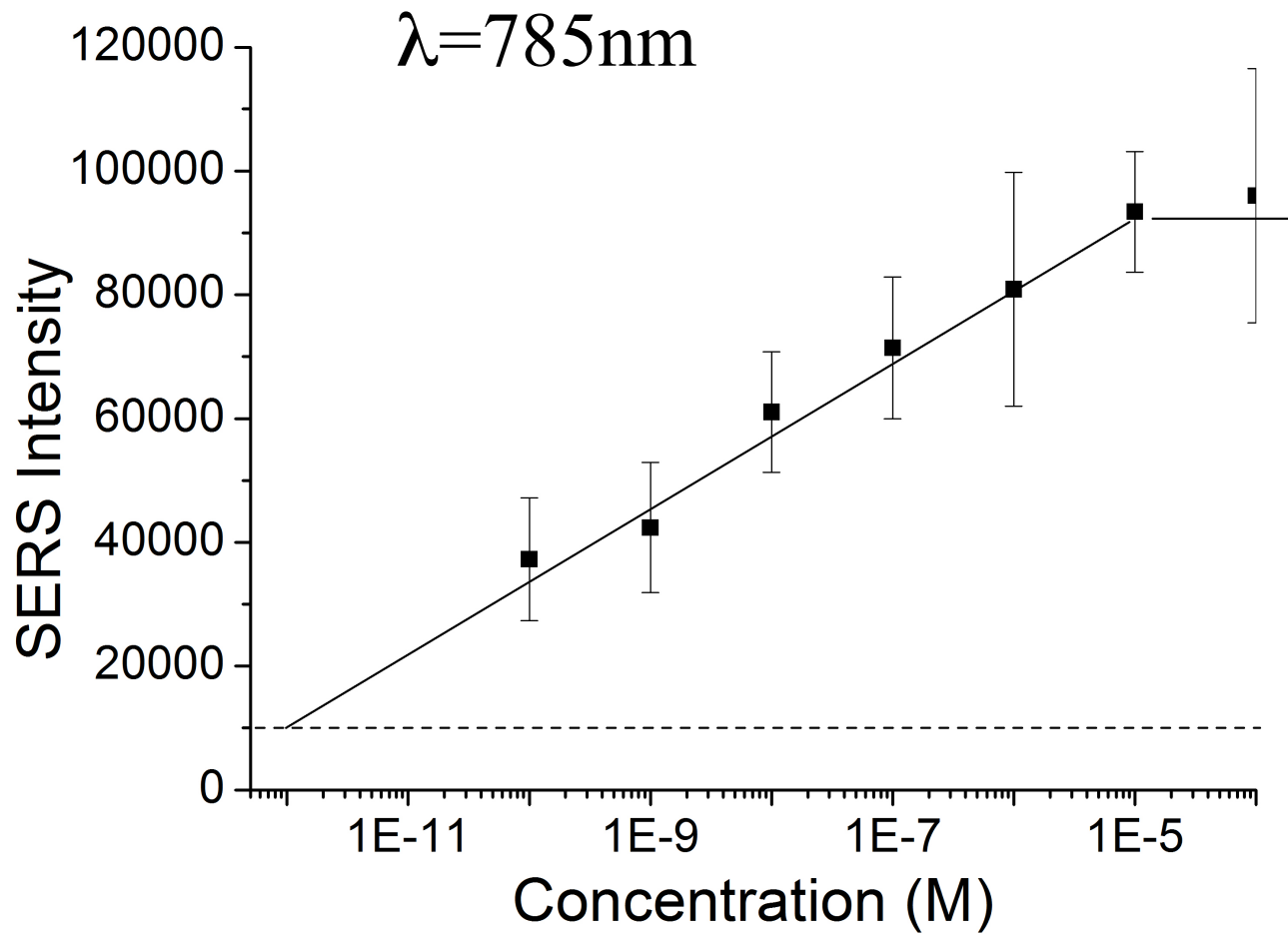
Length = 100 nm

Gap = 20 nm

Benzenethiol
 $\lambda_{\text{exc}} = 785\text{nm}$



Sensor limit of detection



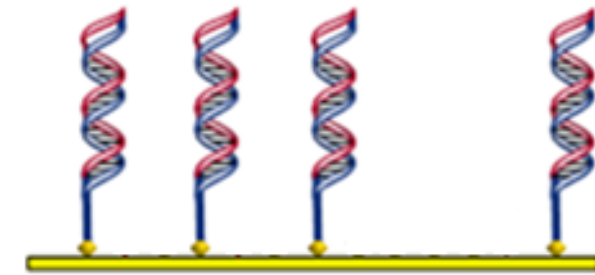
- ➡ At 785 nm, LOD = 1 pM
- ➡ Dimers are two orders of magnitude more sensitive

MnSOD Detection

- Cleaning samples with UV ozone and ethanol
- Aptamer:

deposit **1h** of **c=100 ng/ μ L**

wash with KCl buffer **2x5 min**



- Blocking molecule :

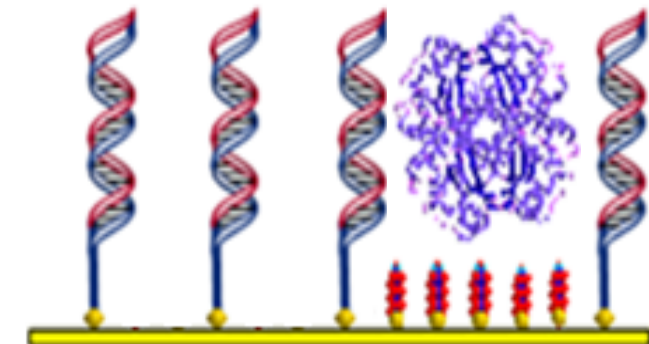
6-Mercapto-1-hexanol

incubation **1h** of **c=2 mM**

wash with ethanol

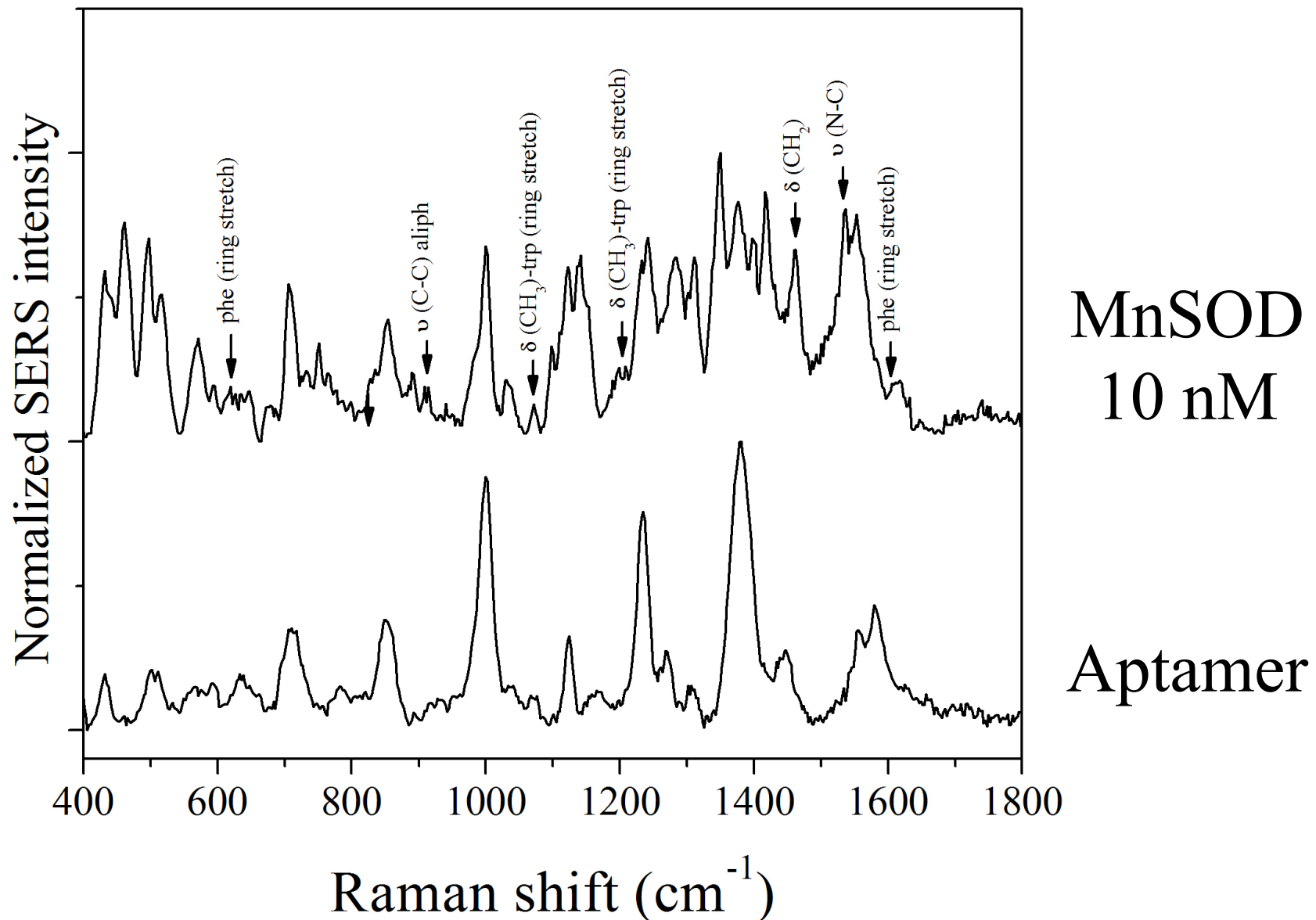
- MnSOD sample: incubation **1h**

Wash with PBS buffer



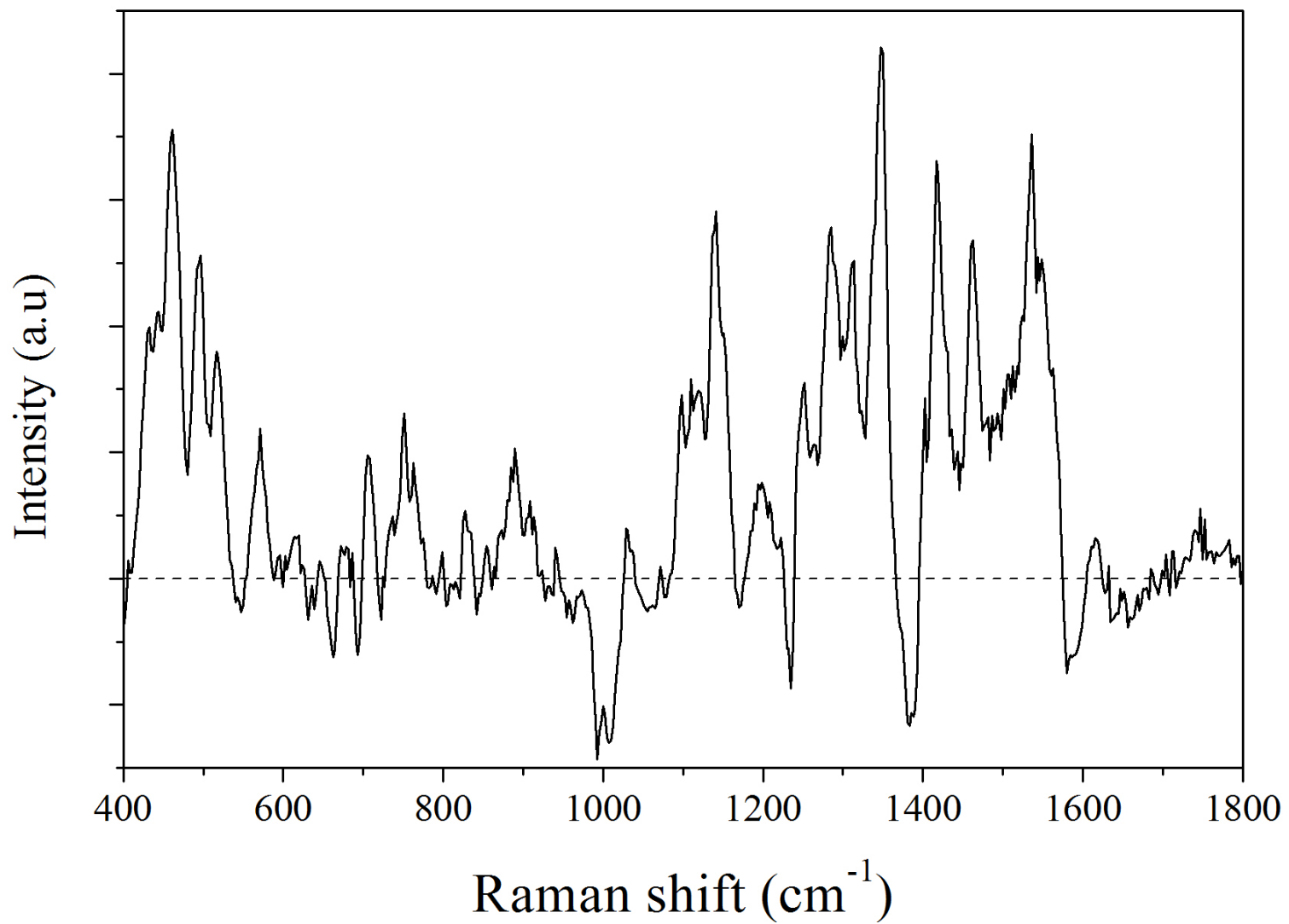
MnSOD Detection: SERS

Laser : **660** nm for $\phi=140$ nm (10s, 0,1 mW)



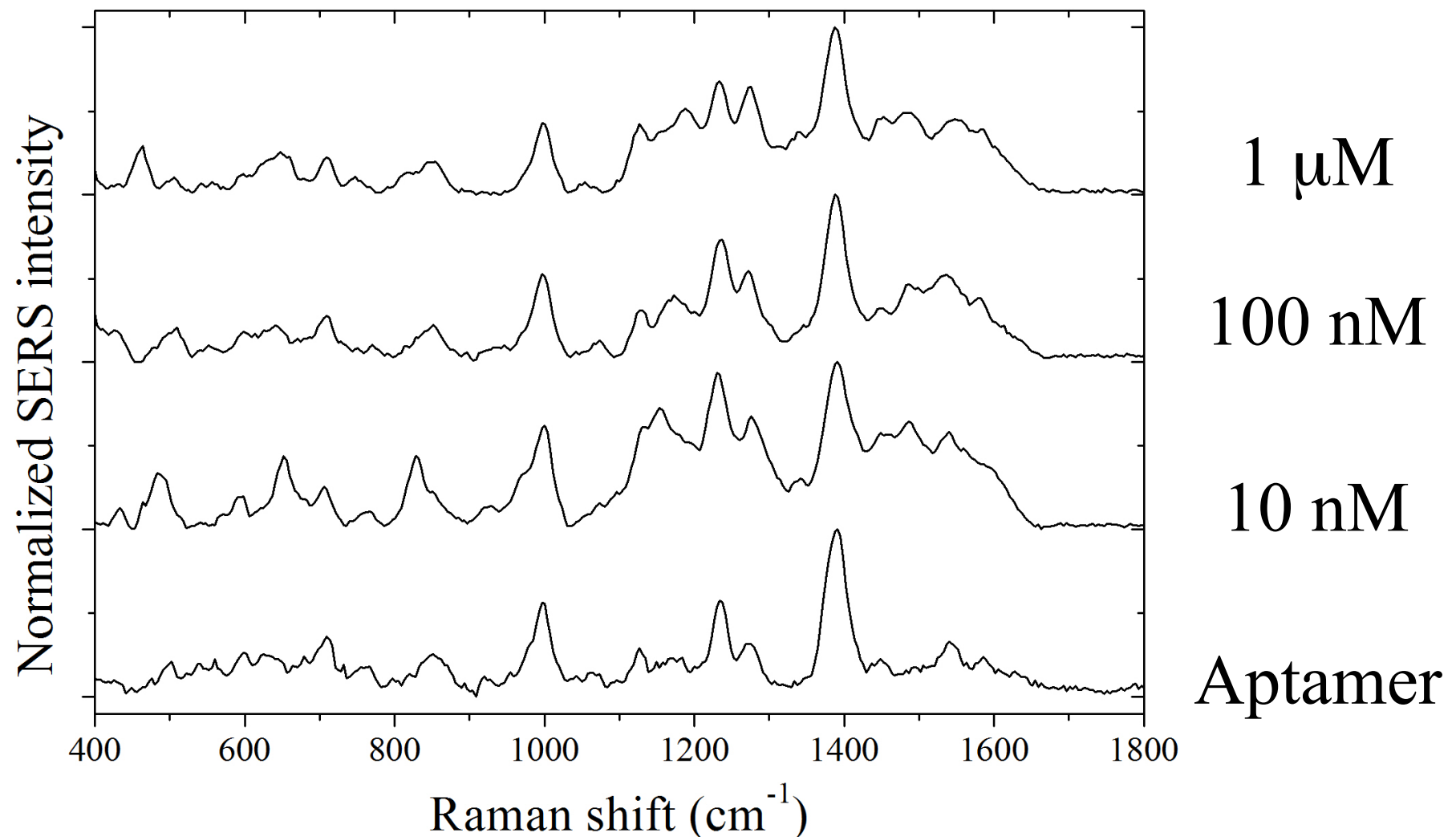
MnSOD Detection: SERS

Laser : **660** nm for $\phi=140$ nm (10s, 0,1 mW)

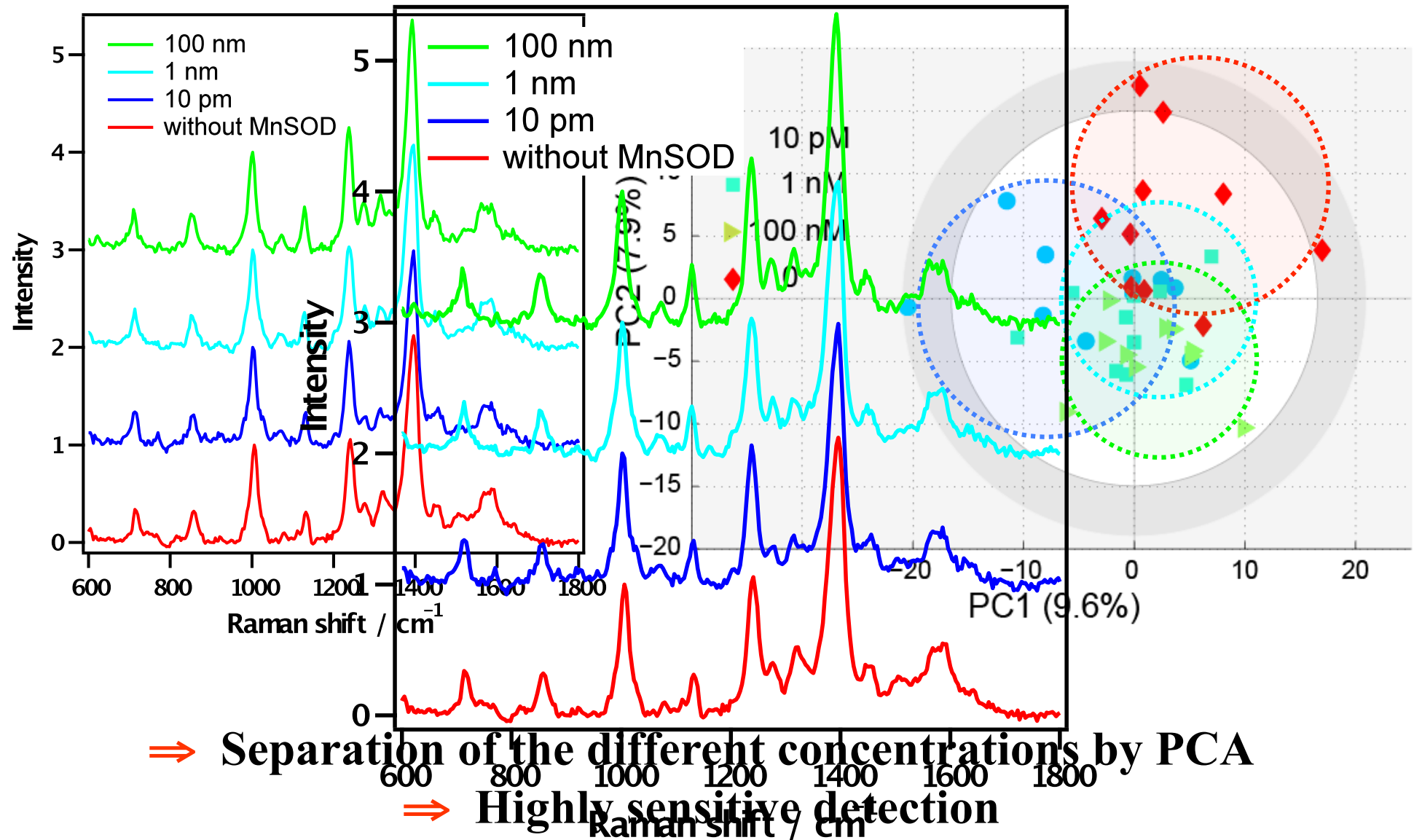


MnSOD Detection: SERS

Laser : **660** nm for $\phi=140$ nm (10s, 0,1 mW)

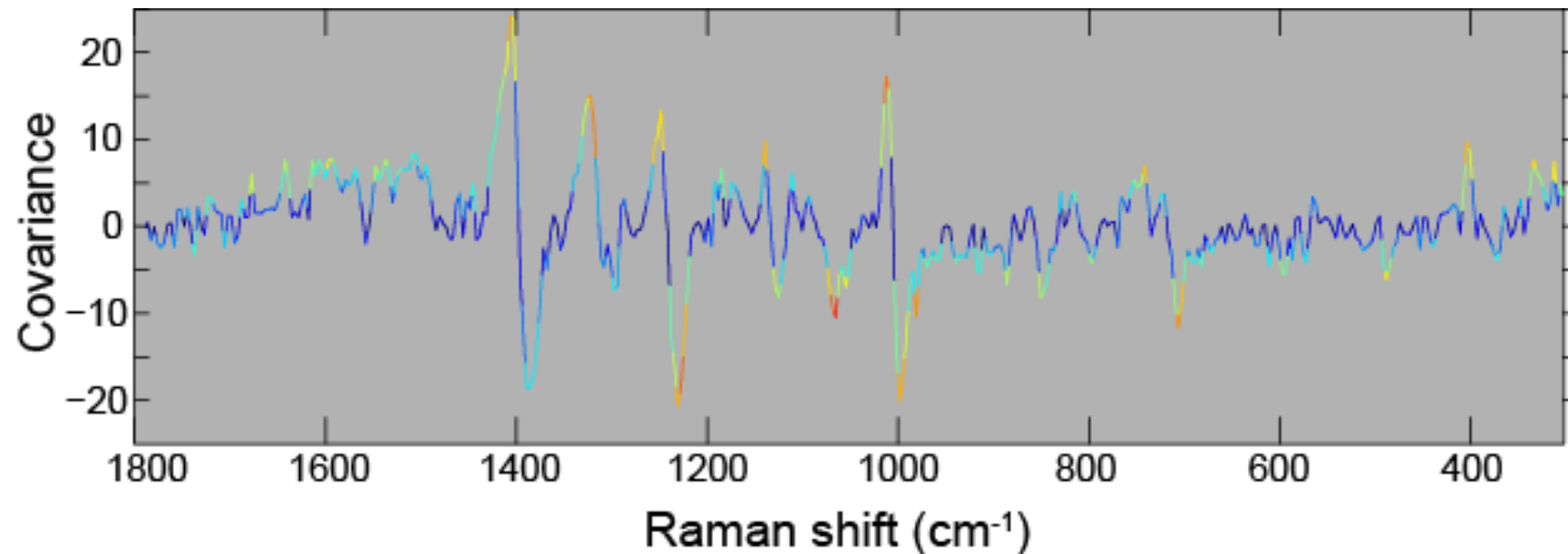


MnSOD Detection: PCA



MnSOD Detection: PCA

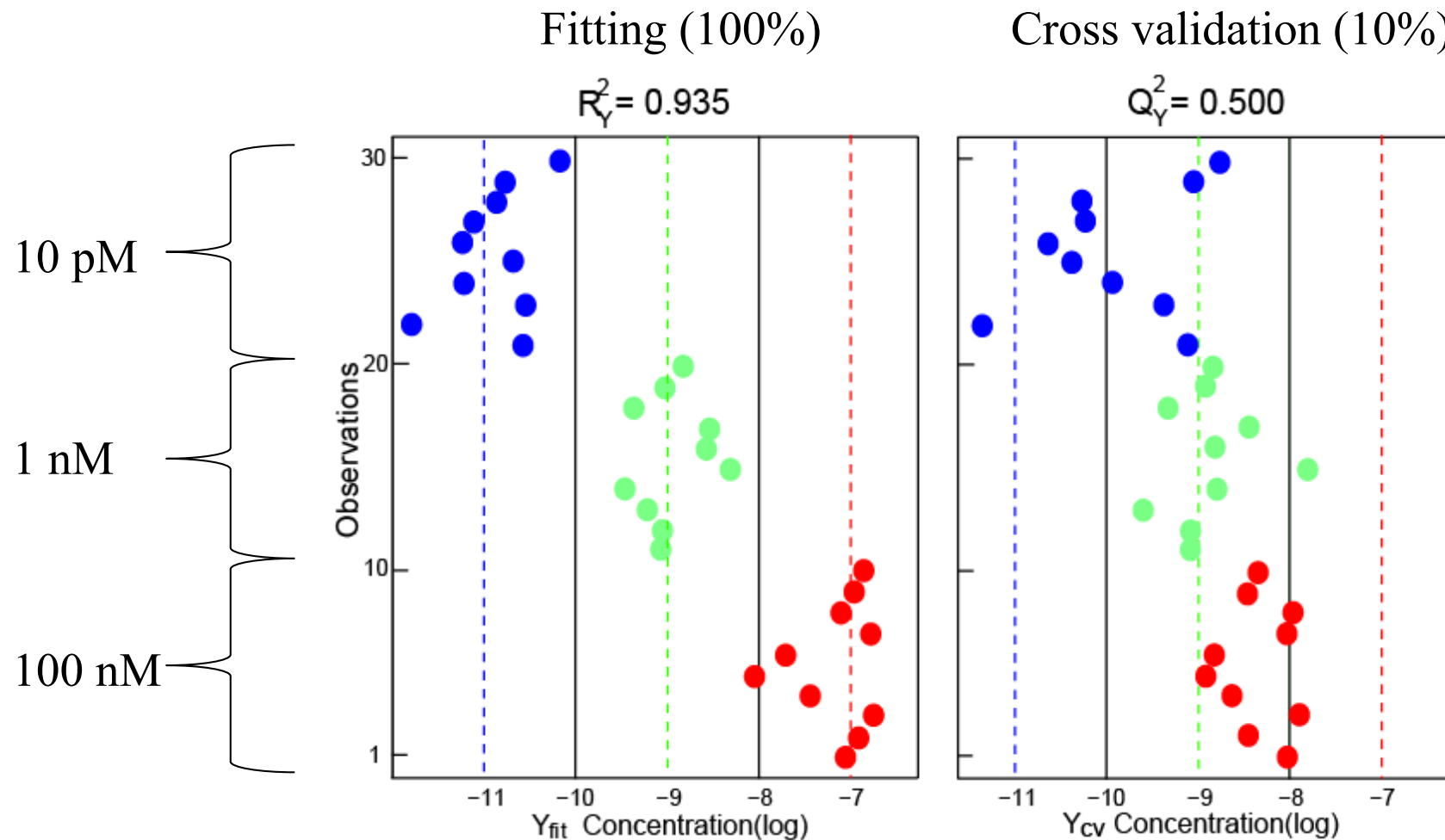
Observation of the spectral variation after the MnSOD deposition



- ➡ Shift of the aptamer bands
- ➡ Modification of the aptamer conformation with MnSOD interaction

MnSOD Detection: PLS

Partial Least Square regression: 30 spectra / 10 per concentration



➡ Discrimination of the different concentrations

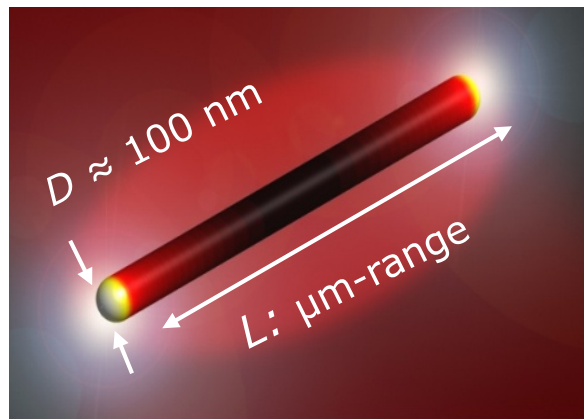
Conclusions

1. Detection limit at the picomolar level
2. Detection of proteins at low concentration
3. Reproducible SERS nanobiosensor

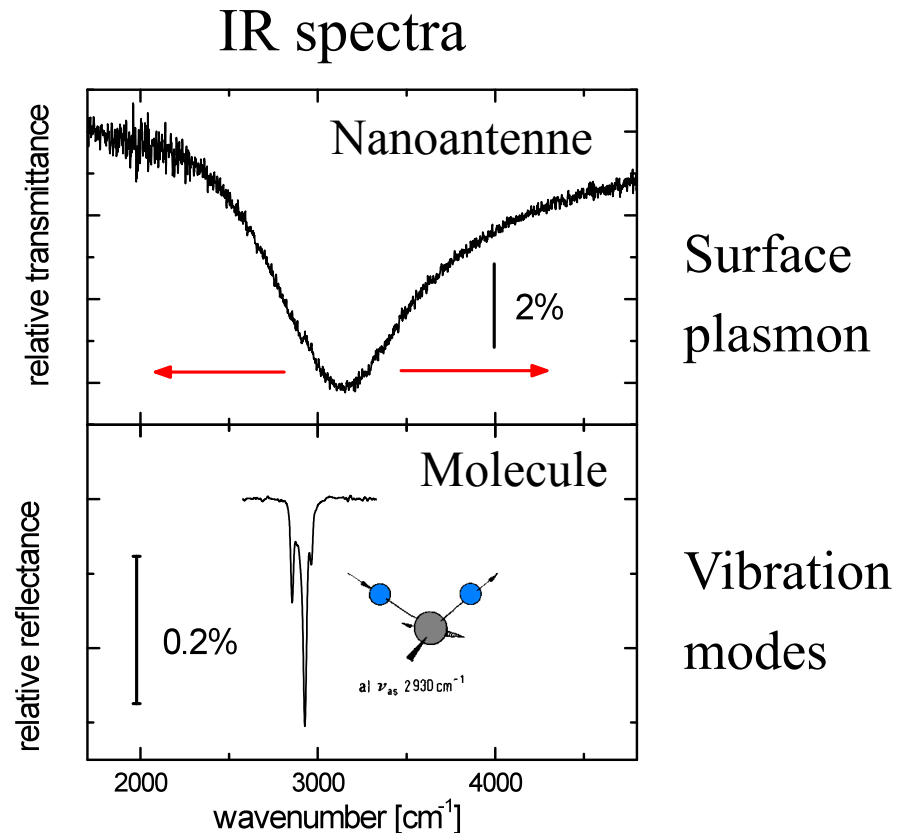
Surface Enhanced IR Absorption

Surface Enhanced IR Absoprtion

Principle : Exploit the near field enhancement created at the nanoantenna vicinity



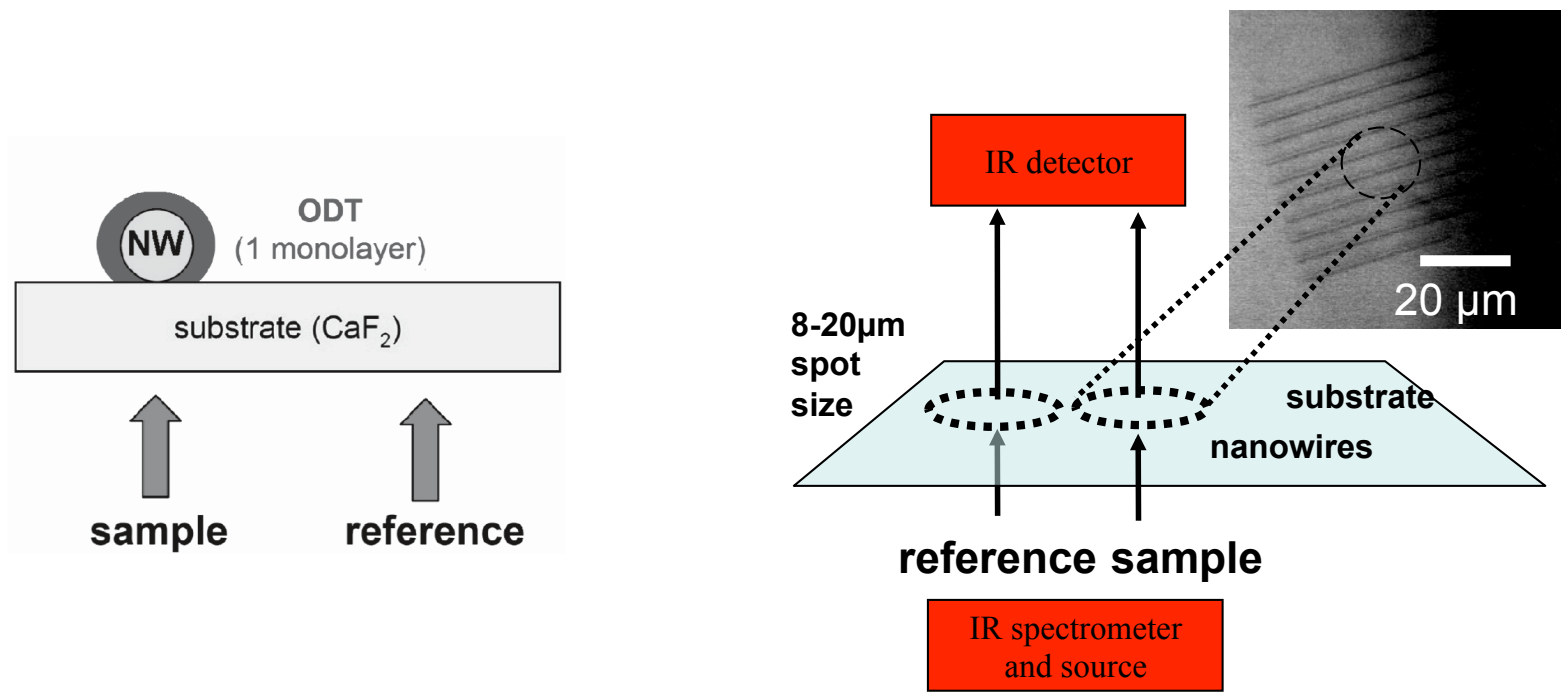
Nanoantenna
- Micrometric length
- Nanometric width



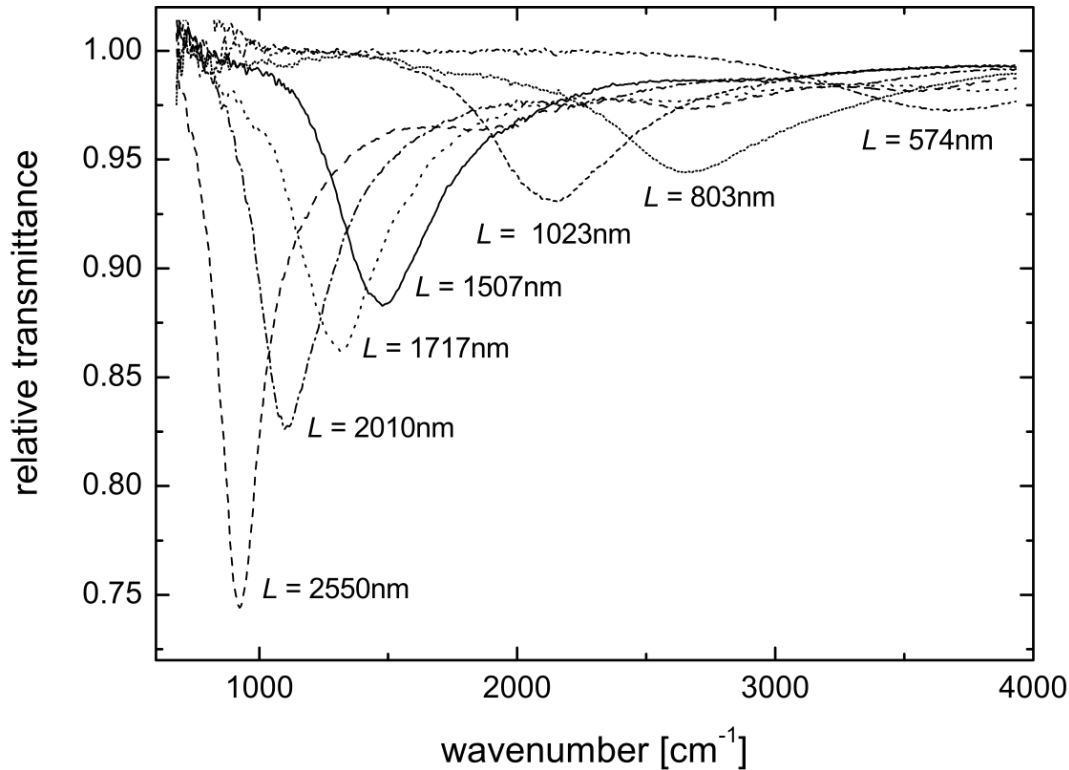
⇒ Coupling between the molecular vibration and the surface plasmon

Surface Enhanced IR Absoprtion

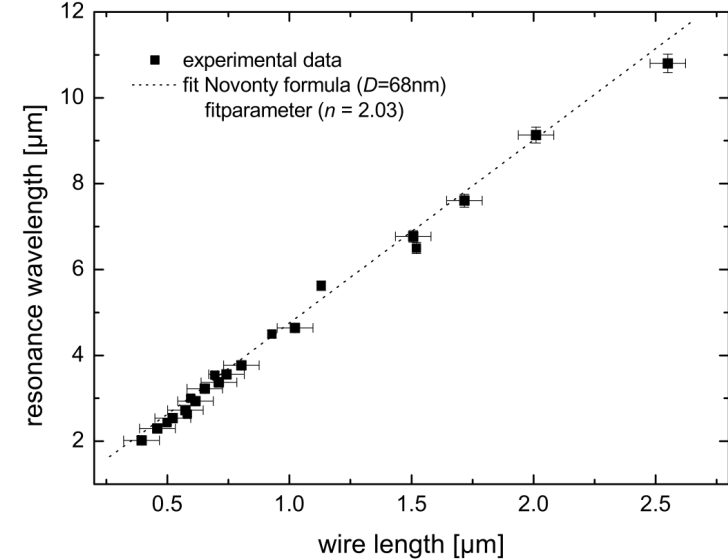
Measurement in transmission with an IR microscope



Surface plasmon in IR



Gold nanowires on ZnS (EBL)
Width and height = 60 nm
Gap = 73 nm



$$2L = a(D, n_{eff}, \lambda_p) \cdot \lambda_{res} \cdot l$$

λ_{res} : resonant wavelength

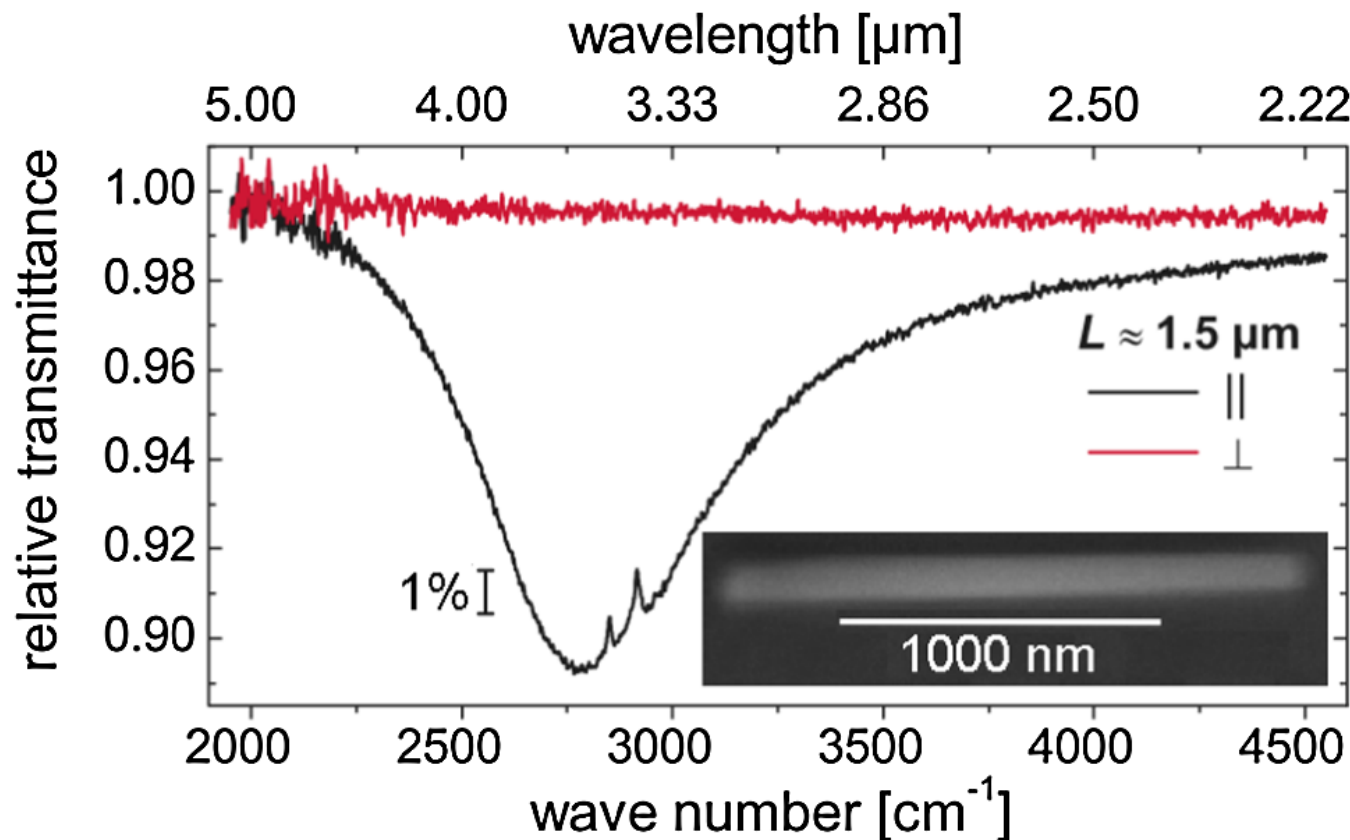
l : order of modes

n_{eff} : effective refractive index

λ_p : plasma wavelength

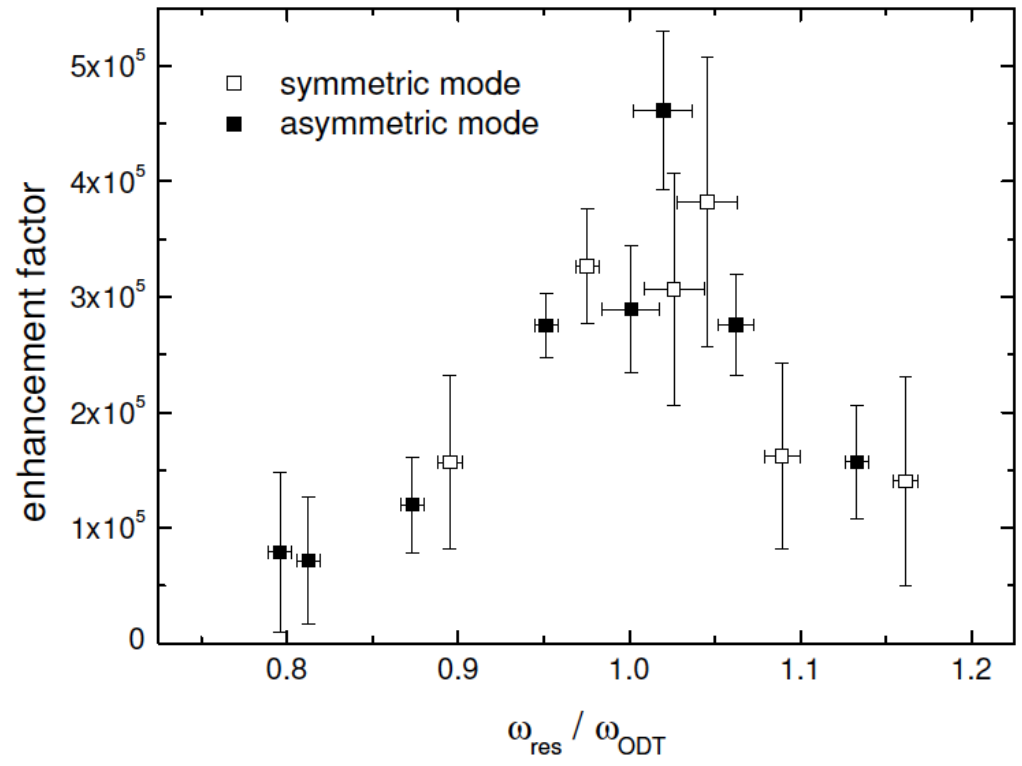
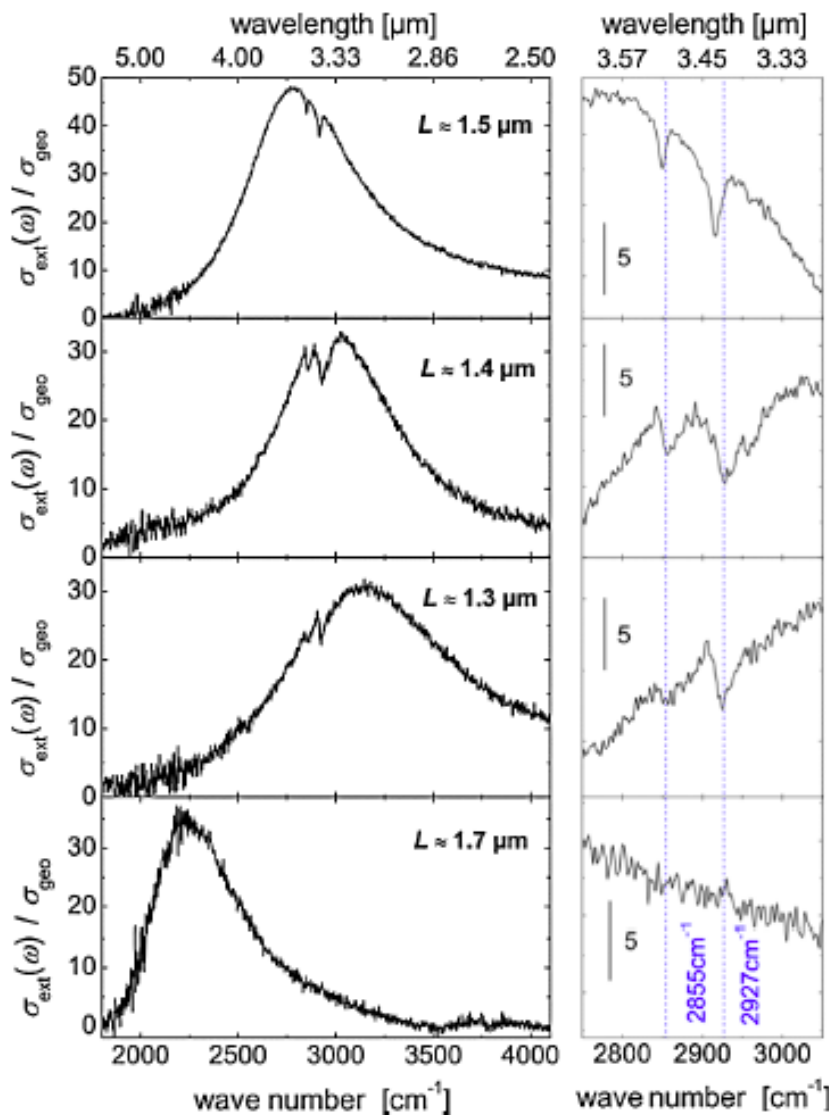
Detection by SEIRA

Gold nanowires on CaF_2 , Electrochemistry on membrane, Diameter = 100 nm
Monolayer of OctaDecaThiol (ODT, C₁₈H₃₇SH)



⇒ Enhancement factor around 300 000

Detection by SEIRA: influence of the LSPR

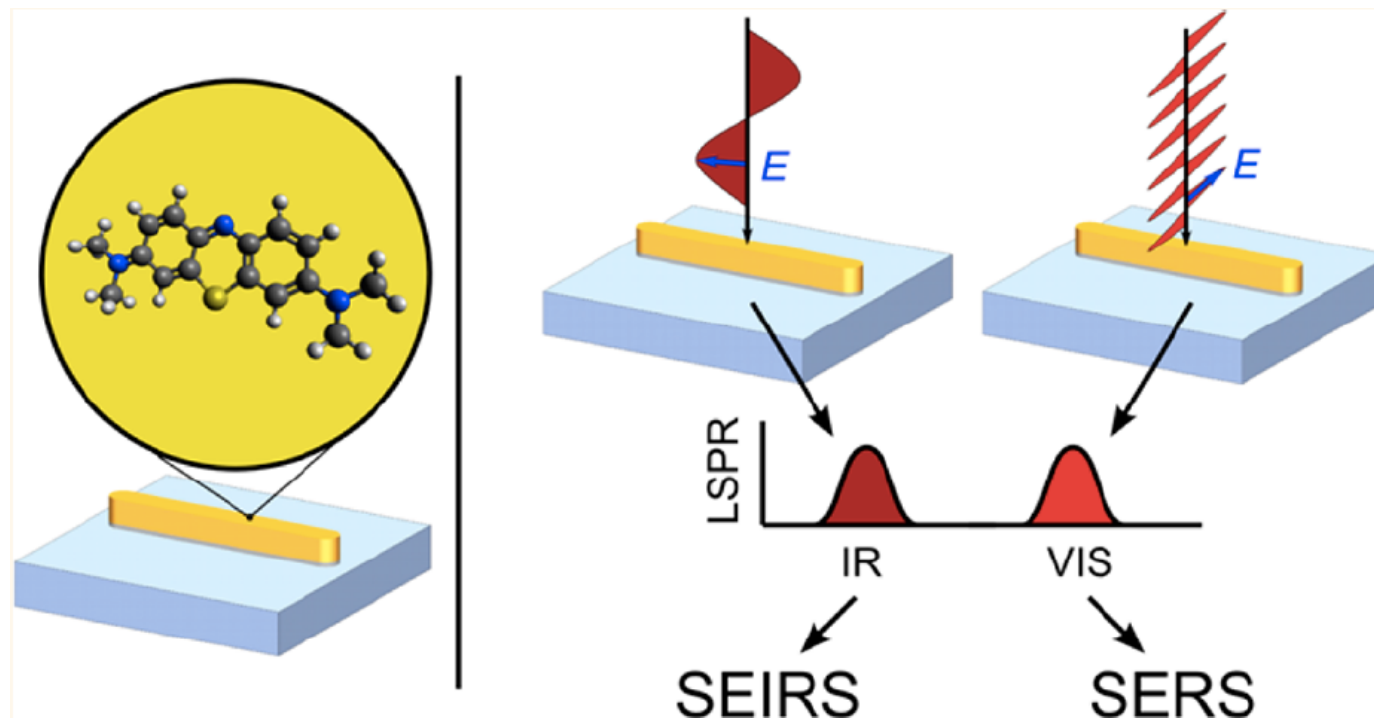


→ Optimal IR signal
for $\lambda_{\text{SPR}} = \lambda_{\text{Vib}}$

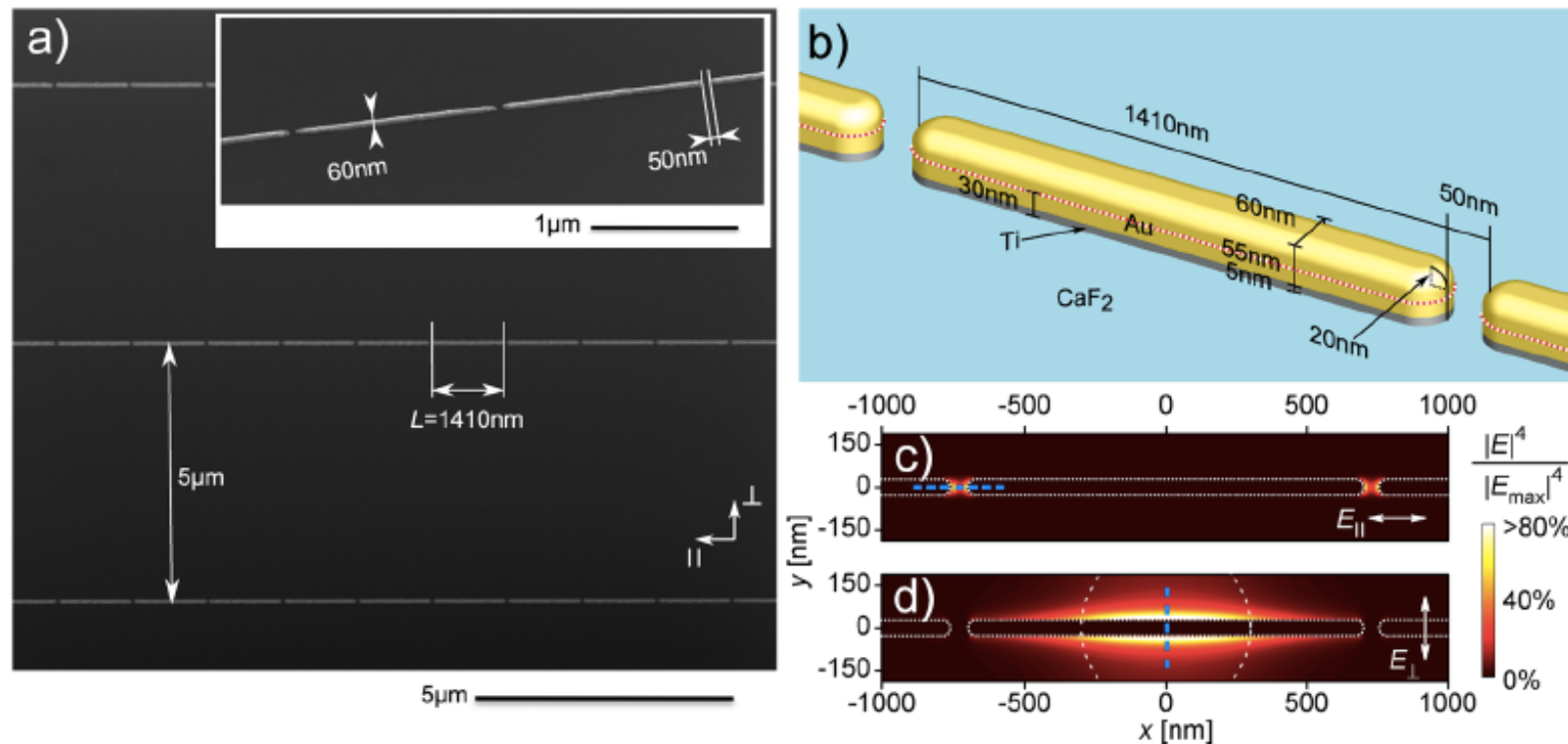
→ Fano behaviour

SERS/SEIRA coupling

SERS/SEIRA: principle

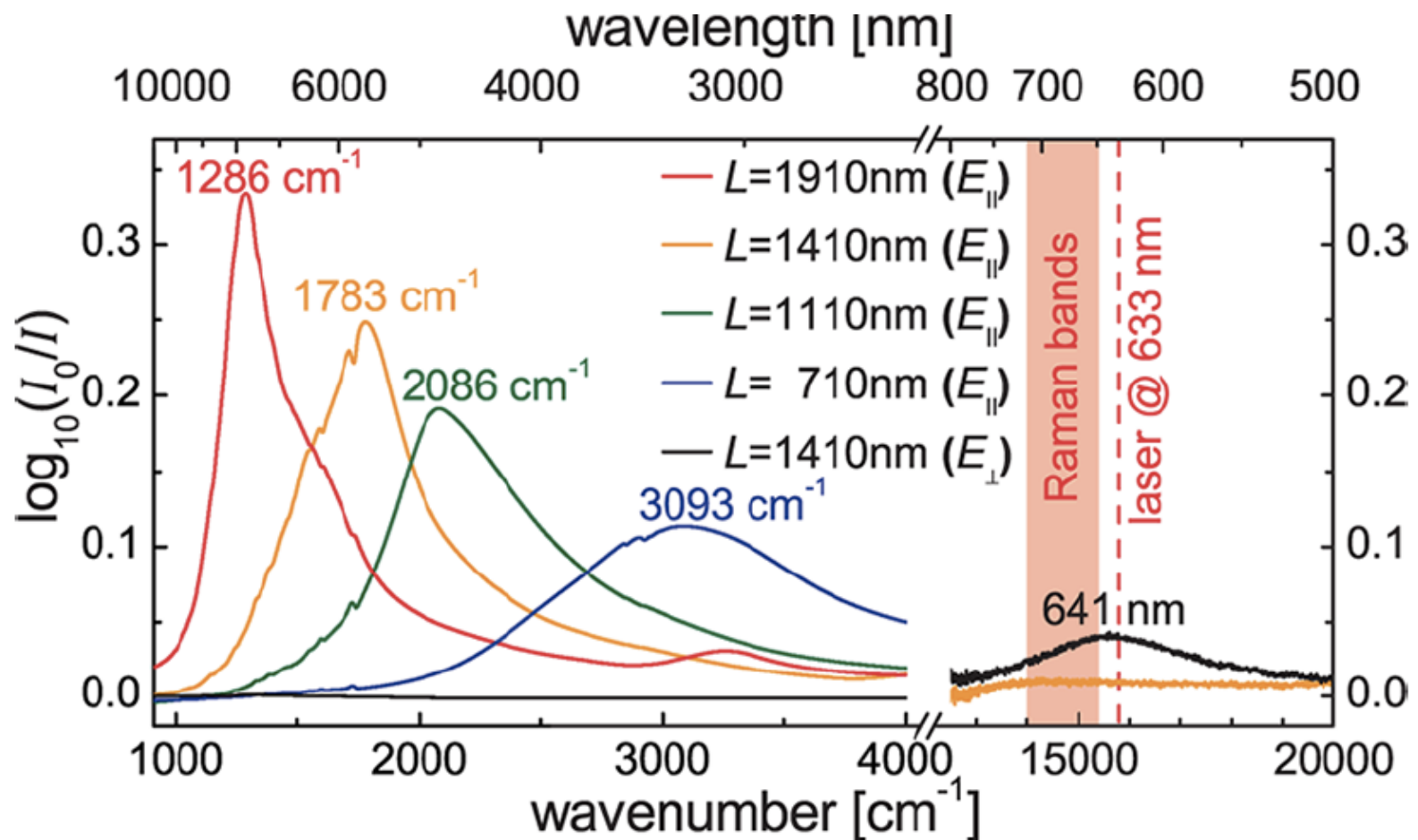


SERS/SEIRA: nanostructures



Methylene blue: 10^{-4} M

SERS/SEIRA: LSPR

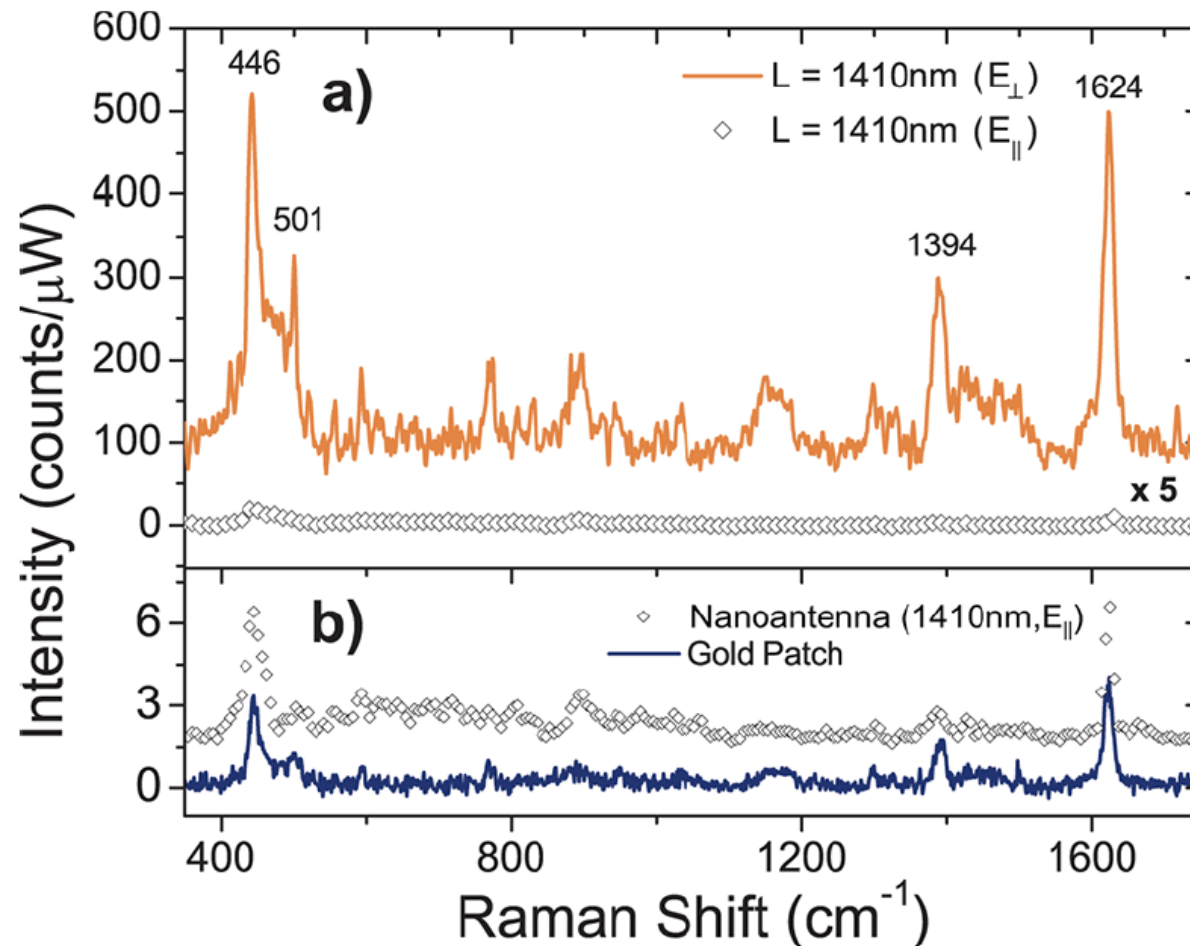


⇒ E_{Para} : Plasmon resonance in IR / SEIRA

⇒ E_{Perp} : Plasmon resonance in the visible / SERS

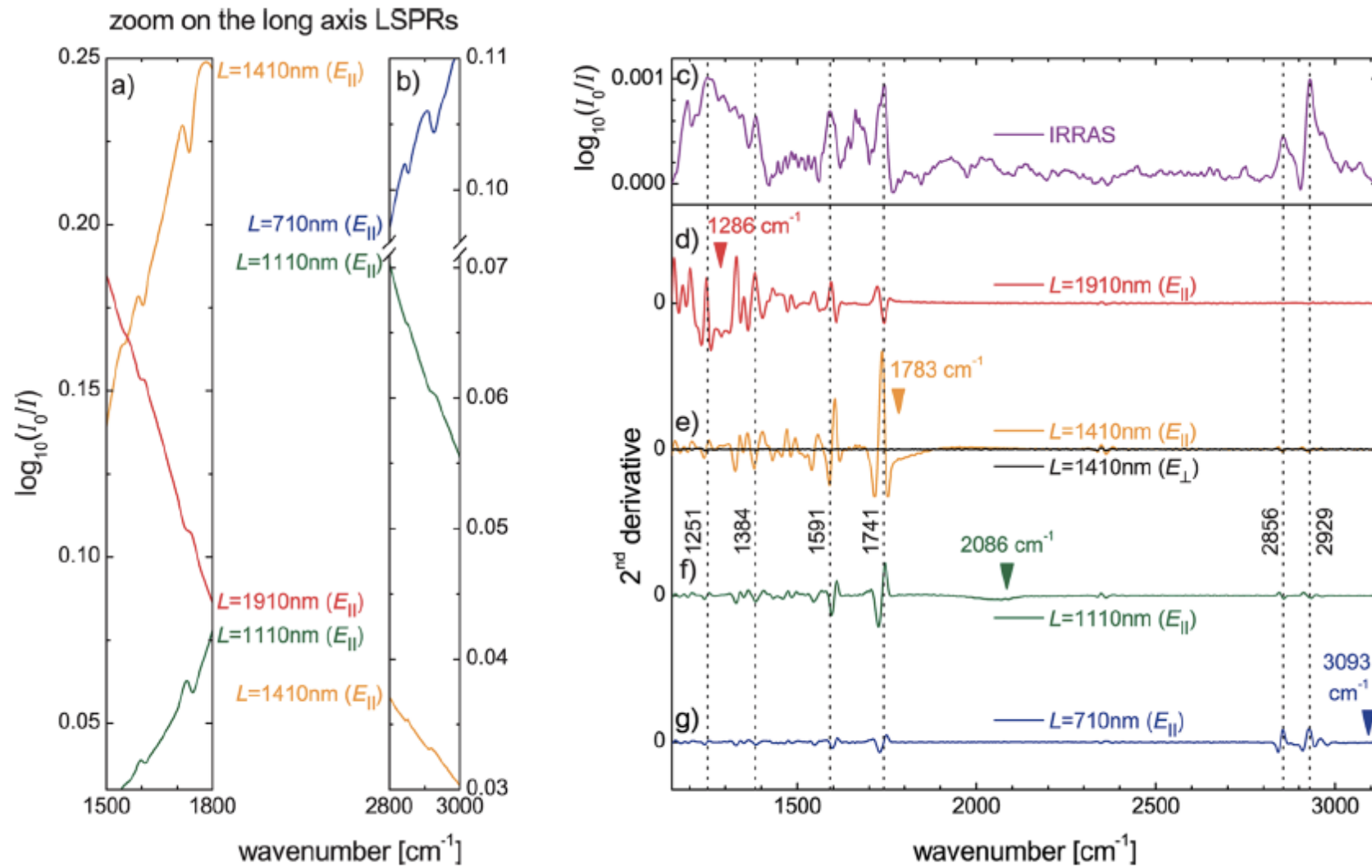
SERS/SEIRA: SERS

HeNe laser : $\lambda = 633$ nm, x100 objective : NA = 0.9



➡ Enhancement factor = 5.10^2

SERS/SEIRA: SEIRA

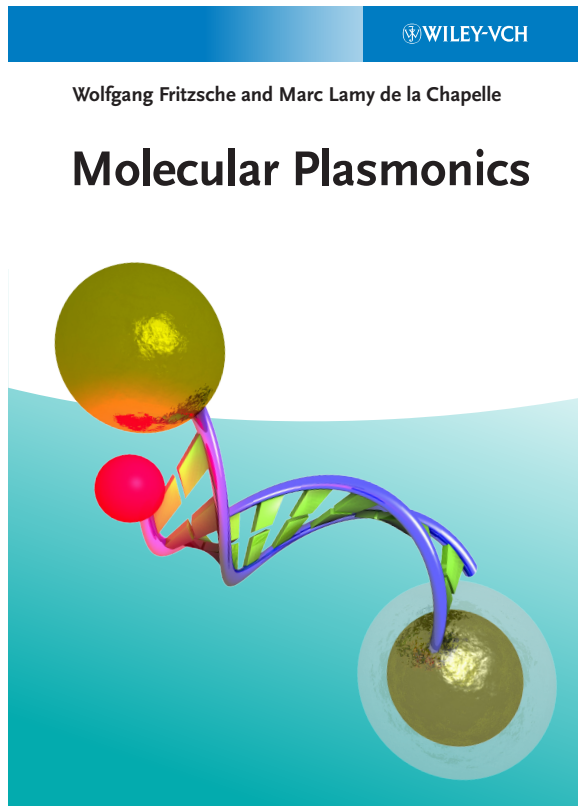


➡ Enhancement factor = 6.10^5

Conclusion

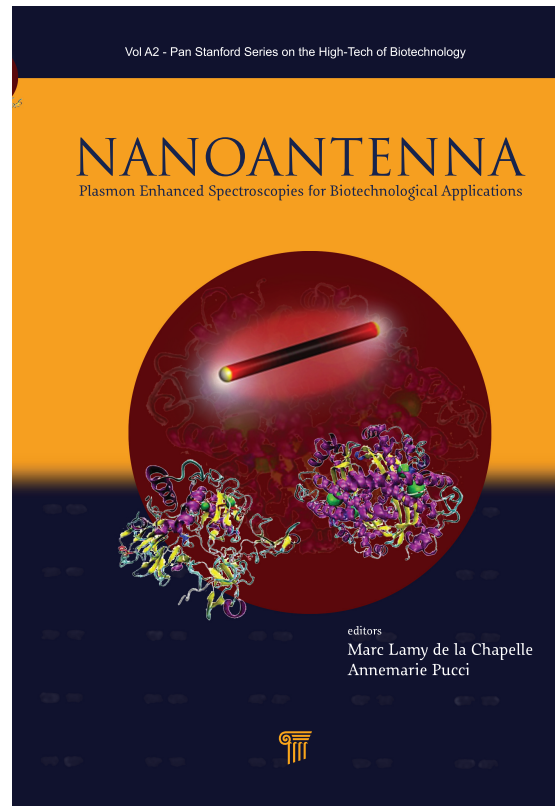
1. Large enhancement factor in SEIRA with nanoantenna
2. Optimisation of the signal in SEIRA
3. SERS and SEIRA coupling with individual nanoantenna

References

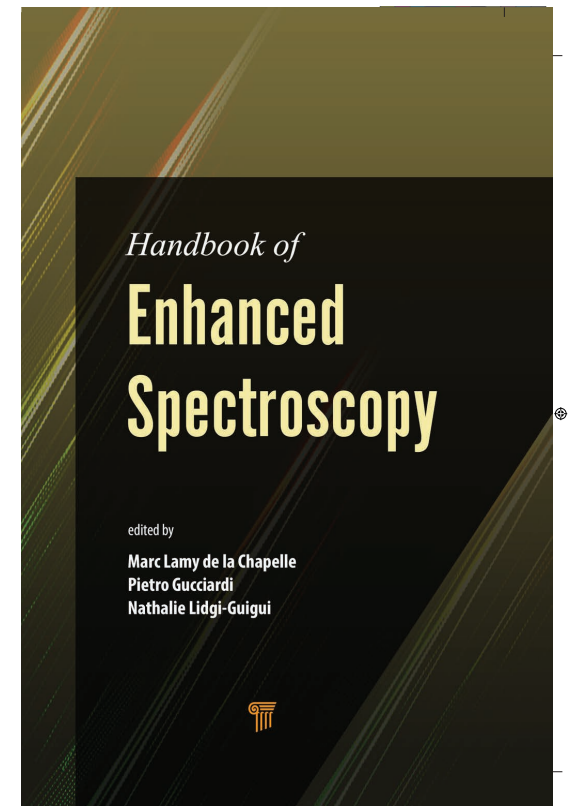


Molecular Plasmonics
W. Fritzsche
M. Lamy de la Chapelle
Wiley VCH Verlag, 2014

Special issue on surface-enhanced Raman spectroscopy
Journal of Optics, Volume 17, Numéro 11, Novembre 2015



Nanoantenna
M. Lamy de la Chapelle,
A. Pucci
Pan Stanford Publishing, 2013



Handbook on Enhanced Spectroscopies
P. Gucciardi,
M. Lamy de la Chapelle,
N. Lidgi-Guigui
Pan Stanford Publishing, 2016

NANOANTENNA European Project HEALTH-F5-2009-241818



REMANTAS and PIRANEX ANR Project



CSPBAT – UMR7244

R. Gillibert
M. Cottat
I. Tijunelyte
N. Guillot
R. Yasukuni
G. Picardi
N. Lidgi
N. Djaker
M. Triba

IPCF - CNR

C. d'Andrea
B. Fazio
P. Gucciardi



ICD-LNIO

J. Ibrahim
H. Shen
T. Toury

N. Malashikhina

R. Grinyté
V. Pavlov



A. Toma
R. P. Zaccaria
E. di Fabrizio

BPC – U1148

H. Hlawaty
A. Sutton
O. Oudar
N. Charnaux



E. Rinnert
F. Colas